Technical Report CHL-99-12
December 1999

US Army Corps of Engineers
Engineer Research and Development Center

Development of Water-Surface Elevation Frequency-of-Occurrence Relationships for the Brunswick, North Carolina, Nuclear Power Plant Site

by Norman W. Scheffner, David J. Mark, Lihwa Lin, Willie A. Brandon, Martin C. Miller

Prepared for U.S. Nuclear Regulatory Commission

The contents of this report are not to be used for advertising, publication, or promotional purposes. Citation of trade names does not constitute an official endorsement or approval of the use of such commercial products.

The findings of this report are not to be construed as an official Department of the Army position, unless so designated by other authorized documents.

Technical Report CHL-99-12
December 1999

Development of Water-Surface Elevation Frequency-of-Occurrence Relationships for the Brunswick, North Carolina, Nuclear Power Plant Site

by Norman W. Scheffner, David J. Mark, Lihwa Lin,
Willie A. Brandon, Martin C. Miller

Coastal and Hydraulics Laboratory
U.S. Army Engineer Research and Development Center
3909 Halls Ferry Road
Vicksburg, MS 39180-6199

Final report

Approved for public release; distribution is unlimited

Prepared for U.S. Nuclear Regulatory Commission
Washington, DC 20314-1000

Army Engineer Research and Development Center Cataloging-in-Publication Data

Development of water-surface elevation frequency-of-occurrence relationships for the Brunswick, North Carolina, nuclear power plant site / by Norman W. Scheffner... [et al.] ; prepared for U.S. Nuclear Regulatory Commission.
81 p. : ill. ; 28 cm. — (Technical report ; CHL-99-12)
Includes bibliographic references.
1. Hydrologic models — North Carolina. 2. Storm surges — Mathematical models. 3. Wind waves — Mathematical models. 4. Brunswick Steam Electric Plant (N.C.) 5. Nuclear power plants — North Carolina. I. Scheffner, Norman W. II. United States. Army. Corps of Engineers. III. U.S. Army Engineer Research and Development Center. IV. Coastal and Hydraulics Laboratory (U.S.) V. U.S. Nuclear Regulatory Commission. VI. Series: Technical report CHL ; 99-12.
TA7 W34 no.CHL-99-12

Contents

List of Figures

List of Tables

Preface

This report summarizes the findings of a comprehensive storm-surge frequency-of-occurrence study conducted for the Brunswick, North Carolina, Nuclear Power Plant. As a part of this analysis, two previous studies were reviewed, one of which provided the design basis flood level of the plant. The second study found that the plant could be susceptible to flooding in the event of an intense hurricane. The purpose of this study is to ascertain, using state-of-the-art modeling and statistical analysis technology, whether the design basis flood level provides an adequate margin of safety for the nuclear power plant. This study was performed by the U.S. Army Engineer Research and Development Center (ERDC) Coastal and Hydraulics Laboratory (CHL), Vicksburg, MS, for the U.S. Nuclear Regulatory Commission. Appreciation is extended to Mr. Robert A. Kornasiewicz of the Structure and Geological Engineering Branch, Division of Engineering Technology, Office of Nuclear Regulatory Research, U.S. Nuclear Regulatory Commission, for his assistance during this study.

The investigation reported herein was conducted by Dr. Norman W. Scheffner, Navigation and Harbors Division (NHD), CHL, and Ms. Willie A. Brandon and Dr. Lihwa Lin, Coastal Hydrodynamics Branch (CHB), NHD. The CHL was formed in October 1996 with the merger of the Coastal Engineering Research Center (CERC) and the Hydraulics Laboratory. Dr. James R. Houston was the Director of CHL, and Mr. Charles C. Calhoun (retired) was the Assistant Director.

Prior to the merger, direct supervision of this project was provided by Mr. H. Lee Butler, Chief, Research Division, CERC, and Dr. Martin C. Miller, Chief, Coastal Oceanography Branch, CERC. After the merger, Mr. C. E. Chatham, Chief, NHD, replaced Mr. Butler as the supervisor. The final report was prepared by Mr. David J. Mark, CHB, and Dr. Scheffner. Ms. Holley Messing, Coastal Processes Branch, CHL, coordinated the report preparation.

At the time of publication of this report, Dr. Lewis E. Link was Acting Director of ERDC, and COL Robin R. Cababa, EN, was Commander.

Conversion Factors, Non-SI to SI Units of Measurement

Non-SI units of measurement used in this report can be converted to SI units as follows:

Multiply	By	To Obtain
feet	0.3048	meters
miles (U.S. statute)	1.609344	kilometers

1 Introduction

To ensure that the safety aspects of a nuclear power plant will not be compromised during severe hurricane surges, the U.S. Nuclear Regulatory Commission (NRC) requires that plants constructed in the coastal zone must be protected to an elevation equal to the surge level induced by the probable maximum hurricane (PMH). The PMH is defined as the most severe storm that is possible, approaching the study area along a critical path and at an optimum rate of movement so as to cause extreme flooding. This hypothetical storm is intended to represent a powerful hurricane whose induced flood levels are estimated to occur once every 2,000 years.

The NRC is presently reassessing the design basis flood level used in protecting the Brunswick, North Carolina, Nuclear Power Plant (BNP), which was established using a PMH-induced storm-surge analysis. A second storm-surge analysis, based on a Joint Probability Method (JPM) found surge levels exceeding the design basis flood level by over 6 ft.[1] Thus, concern exists that this level for the BNP may be too low, possibly subjecting the safety-related equipment at the power plant to flooding induced by an extreme hurricane. The purpose of this study is to determine realistic frequency relationships using state-of-the-art modeling and statistical analysis techniques and to evaluate the PMH-induced surge elevations produced in the two previous studies.

This report describes the procedure and results used in the present hurricane stage-frequency analysis for the BNP using a third statistical technique, the empirical simulation technique (EST). This procedure, used for determining frequency-of-occurrence relationships, is a statistical resampling procedure that uses historical data to develop joint probability relationships among various measured storm parameters (e.g., maximum wind speeds). The resampling scheme generates large populations of data that are statistically similar to a much smaller database of historical events. Using this expanded data set, the EST generates a database of peak storm-surge elevations by simulating multiple-year periods (e.g., 2,000-year periods) of storm activity a multiple number of times. Stage-frequency relationships are then generated using the database of maximum total storm-surge elevations.

Results contained in this study are also compared with those obtained in the previous studies. The present analysis consisted of four interrelated tasks, each

[1] A table of factors for converting non-SI units of measurement to SI units is presented on page vii.

employing a numerical model. In the first task, historical hurricanes impacting the study area were analyzed to determine storm statistics and correlations. From these data, a reduced set of hurricanes, representative of all storms impacting the area, were chosen and subsequently simulated with a tropical wind field model to generate wind and atmospheric pressure fields.

Storm-surge events developed with the wind model output were simulated, in the second task, using a long-wave, finite-element-based hydrodynamic model to obtain peak storm-surge elevations. A spectral wind-wave model was employed to estimate wave setup in the third task.

With the hurricane parameters serving as input to the wind field model, together with the corresponding total storm-surge elevations (combined storm surge, wave setup, and tide) predicted by the various models, statistical techniques are used for developing frequency-of-occurrence relationships in the fourth task.

This report is divided into eight chapters, with Chapter 1 being the introduction. Chapter 2 describes the study area and environmental settings. Chapter 3 describes the EST, whereas Chapter 4 describes the meteorological, wave, and hydrodynamic models applied in this study. Model validation is presented in Chapter 5, and development of the stage-frequency relationships is discussed in Chapter 6. Results obtained in this study are compared with those reported in the two previous studies and presented in Chapter 7. Chapter 8 summarizes the procedures and results of this study. Appendix A contains stage-frequency relationship tables, and stage-frequency relationship figures are presented in Appendix B.

2 Study Site and Environmental Settings

The BNP is located at 33^0 57' 30" north latitude, 78^0 00' 30" west longitude. This position lies near the west bank of the lower Cape Fear River, about 2 miles north of Southport, North Carolina, and 4 miles north of the mouth of the Cape Fear River (Figure 1). Its elevation is approximately 7 m mean sea level (MSL).

The BNP pumps cooling water from the Cape Fear River through a 3-km-long intake canal and releases the effluent to the Atlantic Ocean through a 7-km discharge canal. Figure 1 shows the location of the BNP, the intake and discharge canals, and the ground-elevation contours in the surrounding area.

The lower Cape Fear estuary contains many islands, tidal flats, and dredge-disposal areas. These include Oak Island to the west of the river mouth and Bald Head Island, Smith Island, and Pleasure Island to the east. The average width of the lower Cape Fear River varies from 1 to 4 km. A ship channel, with depth and width of 11 and 150 m, respectively, is maintained by the U.S. Army Corps of Engineers (USACE) in the lower river reach.

The climate of the area is generally mild because of the influence of the ocean and the Gulf Stream located about 70 km offshore. The tide is primarily semi-diurnal, and mean and spring tidal ranges vary from 1.3 to 1.5 m, respectively, at Bald Head Island. Flooding is generally not a problem of major importance in the lower Cape Fear River basin. Most of the largest floods have resulted from storm-induced surges caused by tropical storms or hurricanes. Lowland and marsh area along the riverbank can be subject to infrequent inundation during moderate storm events. In the case of a large hurricane, storm water can overwash Bald Head, Oak, and Smith islands, resulting in a higher storm-surge water level along the lower river reach.

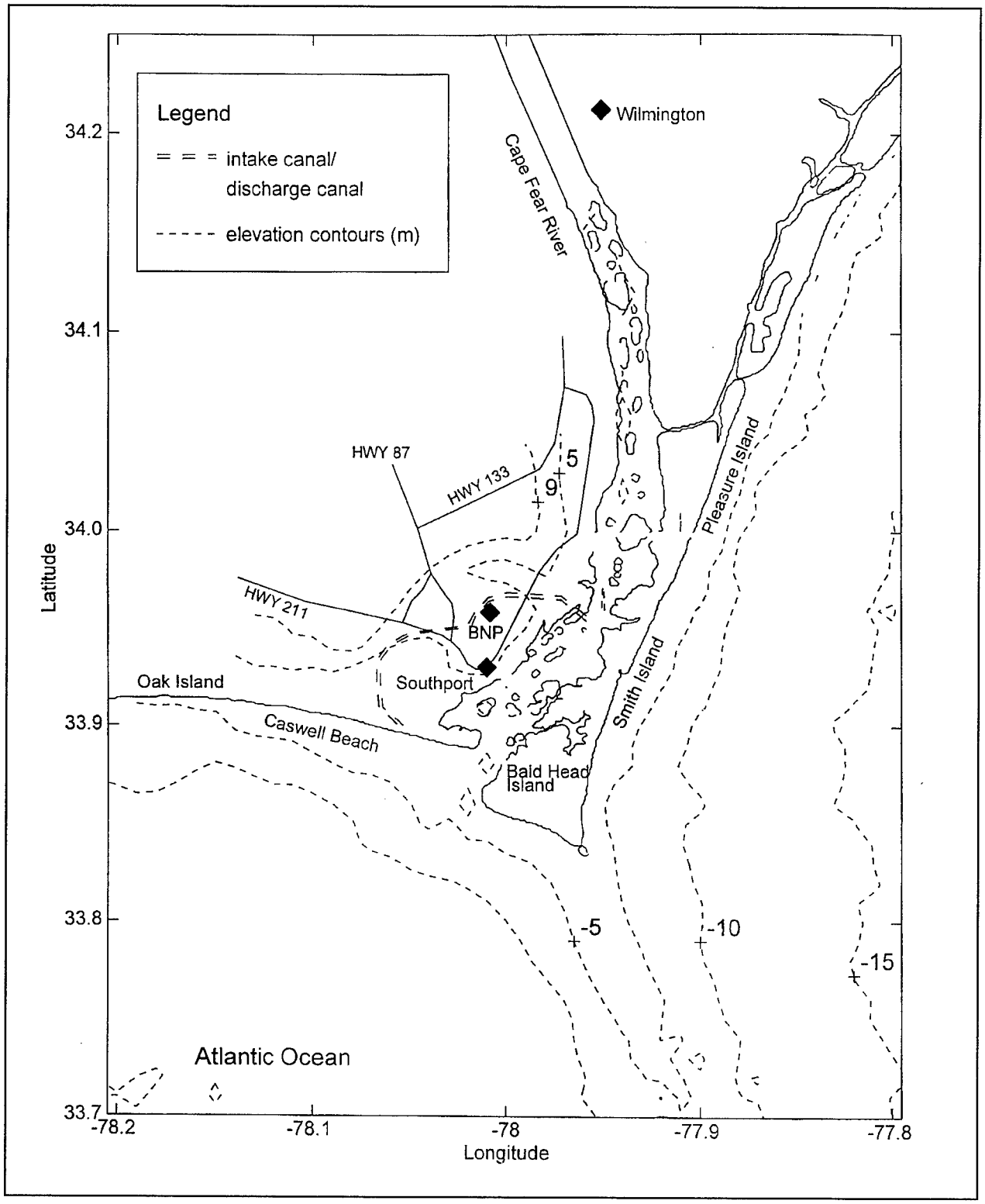

Figure 1. Location and vicinity of the BNP site

3 Empirical Simulation

Technique

Design of structures in areas subject to coastal flooding typically require a storm-surge analysis to obtain a peak water-surface elevation for defining the minimum elevation at which the structure can be built. Frequently, standard ranking methods cannot be used in a stage-frequency analysis because of the lack of measured peak storm-surge stages at a given site. Consequently, numerical models are often applied for simulating storm-surge events for estimating peak storm-surge stages. Traditionally, modeled hurricanes are synthesized via a JPM to describe storm parameters, such as maximum wind speeds and pressure deficits. First employing a statistical analysis of historical storms to determine probability density functions (pdfs) for storm parameters, several values for each parameter are then chosen (together with their associated probability of occurrence) from its pdf. Next, a series of hypothetical hurricanes are synthesized by combining various parameter values. The probability of occurrence for each storm is the product of the probability of occurrence of each parameter composing that storm, multiplied by the frequency of occurrence of hurricanes in the study region.

One shortcoming of this approach, however, is that the JPM usually assumes that all parameters are independent, ignoring the interdependence of storm parameters. Consequently, unrealistic hurricanes are synthesized by arbitrarily combining parameter values. For example, hurricanes having higher pressure deficits also experience higher rotational velocities, whereas lower pressure deficits result in slower rotational velocities. With the JPM, a synthesized storm could be constructed with a higher pressure deficit parameter value and a slower rotational velocity parameter value, resulting in an unrealistic storm.

Furthermore, assuming parameter independence may lead to an overestimated probability of occurrence for a synthetic storm; should this storm be extreme, higher flood elevations will be predicted for a particular return period than are warranted by the historic data. This phenomena can be illustrated in the following hypothetical (and much simplified) example: a stage-frequency analysis is performed at a particular site where 25 hurricanes have impacted this site over a 100-year period. For convenience, only two parameters, track direction and pressure deficit, are used in developing an ensemble of synthetic storms. A review of the historic data shows that the storms track in only the northeast and

northwest directions, and that these tracks have an equal probability of occurrence (i.e., 50 percent each). Further assume that the pressure deficits for those storms tracking towards the northwest range from 80 to 120 mb, whereas pressure deficits range from 40 to 80 mb for those hurricanes with northeasterly headings.

Imposing parameter independence and developing a pdf for the pressure deficit parameter (where deficits from all storms, regardless of track, are used in developing the pdf), five deficit values are then selected together with their (assumed) associated probabilities, which are 40 mb (5 percent), 60 mb (25 percent), 80 mb (40 percent), 100 mb (25 percent), and 120 mb (5 percent). In this scenario, 10 storms comprise the ensemble, where five storms have a northeasterly heading with pressures ranging from 40 to 120 mb, and another five having the same pressure deficits but with a northwesterly heading. Comparing the synthetic with the historic storms shows that 4 of the 10 storms in the ensemble are not representative of historic events. (These storms are the two with pressure deficits of 100 and 120 mb and a northeasterly heading and the two northwesterly storms with the 40 and 60 mb pressure deficits.)

In addition to not being representative of historic events, the probabilities associated with these storms are not accurate. For example, the northeasterly storm with a pressure deficit of 120 mb would be assigned a probability of occurrence of 0.0063 (i.e., Pr[track] $\times$ Pr[pressure] $\times$ frequency of occurrence of all hurricanes impacting the site, or $0.50 \times 0.05 \times 25/100$) using the JPM. Because the probability of occurrence assigned to this pressure deficit stems primarily from those storms with a different track, and since no historic storm having this extreme deficit occurred, the probability is overestimated. Although a storm having these parameters may occur in the future, its probability is unknown; one must conclude that its probability must be lower because no event of this intensity has occurred. Thus, a level of uncertainty is incorporated into the stage-frequency computations. An alternative approach to the JPM is the EST or extended "bootstrap" approach, which preserves the interdependence of hurricane parameters. Details of the EST are given in Scheffner and Borgman (1992) and Borgman et al. (1992).

EST is a statistical resampling, nearest neighbor, random-walk interpolation technique that uses historical data to develop joint probability relationships among the various measured storm parameters. In contrast to the JPM discussed above, there are no simplifying assumptions concerning the development of pdfs describing historical events. Thus, the interdependence of parameters is maintained. In this manner, parameter probabilities are site specific, do not depend on fixed parametric relationships, and do not assume parameter independence. Thus, the EST is distribution free and nonparametric. The only assumption in the EST is that future events will be statistically similar in magnitude and frequency to past events.

For this study, the EST was developed to generate numerous multiyear intervals of possible future hurricane events for a specific location. The ensemble of modeled or simulated events is consistent with the statistics and correlations of past storm activity at a site. Furthermore, the EST permits random deviations in

storm behavior (when compared with historic events) that could occur in the future. For example, simulated hurricanes are permitted to make landfall at locations other than those made by the historical storms. These random deviations can also result in more intense storms than the historical events themselves, allowing for the possibility of a future hurricane being the storm of record.

The simulation approach requires specifying a set of parameters that describe the dynamics of some physical system, such as hurricanes. These parameters, which must be descriptive of both the process being modeled and the effects of that process, are defined as an N-dimensional vector space. The parameters that describe only the physical attributes of the process are referred to as input vectors.

In the case of hurricanes, pertinent input vectors include central pressure deficit, radius to maximum winds, maximum winds, minimum distance from the eye of the storm to the location of interest, forward speed of the eye, and tidal phase during the storm event. These values, as they will later be described, can be defined for each specific location corresponding to each particular historical event of the total set of events used in the study.

The second class of vectors involves some selected response resulting from the N-dimensional, parameterized storm. For hurricanes, response vectors can include maximum storm surge, shoreline erosion, dune recession, or any other response that can be attributed to the passage of a storm. For this study, the maximum total water-surface elevation, reflecting the combined contributions of storm surge, wave setup, and tide, is the response vector of interest.

Although response vectors are related to the input vectors, the interrelationship is highly nonlinear and involves correlation relationships that cannot be directly defined, i.e., a nonparametric relationship. For example, in addition to the storm input parameters, storm surge is a function of local bathymetry, shoreline slope and exposure, ocean currents, temperature, etc., as well as their spatial and temporal gradients. It is assumed, however, that these combined effects are reflected in the response vector. For the case of storm surge in the vicinity of the BNP, wave and hydrodynamic models are used for computing response vectors as a function of the storm parameters (i.e., input vectors), local bathymetry, and shoreline configuration. Other response vectors such as sediment transport, shoreline response, and dune recession require application of additional models.

From this historical data set a subset of storm events is selected that is representative of the entire set of historical storms. This subset is referred to as the "training set." Furthermore, those storms comprising the training set are subsequently used as input to appropriate numerical models for computing the desired response vectors. The training set usually includes historical events but may include historical storms with a deviation or perturbation, such as a hurricane with a slightly altered path. Some historical events may also be deleted from the training set if two events are nearly identical such that both would produce the same response. Because the purpose is to fill the parameter space, two similar events are redundant.

The training set can be augmented with additional storms contained in the historical data set. Storm events augmenting the training set are referred to as the "statistical set" of storms. Whereas numerical models are used for generating response vectors for those events in the training set, response vectors for the statistical set of storms are interpolated using the training set response vectors. Thus, stage-frequency relationships can be generated using the entire historical data set without need of simulating all storms in that data set.

With the augmented storm data set (i.e., training and statistical storm sets), the EST produces N simulations of a T-year sequence of events (hurricanes), each with their associated input vectors and response vectors. Because there are N-repetitions of a T-year sequence of events, an error analysis of the results can be performed with respect to median, worst, least, standard deviations, etc. The following describes the procedures by which the input and response data are used to produce multiple simulations of multiple years of events.

Two criteria are required of the T-year sequence of events. The first criterion is that the individual events must be similar in behavior and magnitude to historical events, i.e., the interrelationships among the input and response vectors must be realistic. The second criterion is that the frequency of storm events in the future will remain the same as in the past. The following sections describe how these criteria are preserved.

Storm-Event Consistency

The first major assumption in the EST is that future events will be similar to past events. This criterion is maintained by ensuring that the input vectors for simulated events have similar joint probabilities as those in the training set. For example, a hurricane with a large central pressure deficit and low maximum winds is not a realistic event; the two parameters are not independent although their precise dependency is unknown. The simulation of realistic events is accounted for in the nearest neighbor interpolation, bootstrap, resampling technique developed by Borgman et al. (1992).

The basic technique can be described in two dimensions as follows. Let X_1, X_2, X_3, ..., X_n be n independent, identically distributed random vectors (i.e., storm events), each having two components $[\boldsymbol{X}_i = \{\underline{x}_i(1), \underline{x}_i(2)\}; i = 1,n]$ (i.e., storm parameters such as pressure deficit and wind speeds).

Each event X_i has a probability p_i as $1/n$; therefore, a cumulative probability relationship can be developed in which each storm event is assigned a segment of the total probability ranging from 0 to 1. If each event has an equal probability, then each event is assigned a segment s_j such that $s_j \rightarrow X_j$. Therefore, each event occupies a fixed portion of the 0 to 1 probability space according to the total number of events in the training set, which can be defined mathematically as:

$$\left[0 < s_1 \leq \frac{1}{n}\right]$$
$$\left[\frac{1}{n} < s_2 \leq \frac{2}{n}\right]$$
$$\left[\frac{2}{n} < s_3 \leq \frac{3}{n}\right] \qquad (1)$$
$$\left[\frac{n\text{-}1}{n} < s_n \leq 1\right]$$

A random number from 0 to 1 is selected and used to identify a storm event from the total storm population. The procedure is equivalent to drawing and replacing random samples from the full storm-event population.

The EST is not simply a resampling of historical events technique, but rather an approach intended to simulate the vector distribution contained in the training set population. The EST approach is to select a sample storm based on a random number chosen from the range of 0 to 1 and then perform a random walk from the selected event X_i (with x_1 and x_2) vectors to the nearest neighbor vectors. The walk is based on independent uniform random numbers ranging from -1 to 1 and has the effect of simulating responses that are not identical to the historical events themselves, but are similar to those events that have historically occurred.

Storm-Event Frequency

The second criterion to be satisfied is that the total number of storm events selected in the T-years must be statistically representative to the number of historical events that have occurred at the area of interest. Given the mean frequency of storm events for a particular region, a Poisson distribution is used to determine the average number of expected events in a given year. For example, the Poisson distribution can be written in the following form:

$$Pr(s;\lambda) = \frac{\lambda^s e^{-\lambda}}{s!} \qquad (2)$$

for $s = 0,1,2,3,....$ The probability $Pr(s;\lambda)$ defines the probability of having s events per year where λ is a measure of the historically based number of events occurring per year. At the BNP site, 24 events occurred over a 111-year period; thus, λ is equal to 0.2162 (i.e., 24/111).

A 10,000-element array is initialized to the above Poisson distribution. The probability corresponding to $s = 0$ storms per year, or no storms occurring in a particular year, is 0.8056; thus, if a random number selection is less than or equal

to 0.8056 on an interval of 0 to 1, then no hurricanes would occur during that simulation year. If the random number falls between 0.8056 and 0.9798 (where the latter value, 0.9798, is found by adding $Pr[s = 0]$ and $Pr[s = 1]$ together, or 0.8056 + 0.1742), one event is selected. Two events are simulated if a random number is selected within the range of 0.9798 and 0.9986 (where 0.9986 = $Pr[s = 0] + Pr[s = 1] + Pr[s = 2]$ = 0.8056 + 0.1742 + 0.0188), etc. When one or more storms are indicated for a given year, they are randomly selected using the nearest neighbor interpolation technique described above.

Output from the EST program is N repetitions of T-years of simulated storm-event responses. It is from these responses that frequency-of-occurrence relationships are computed. The computational procedure followed is based on the generation of a probability distribution function corresponding to each of the T-year sequence of simulated data.

Recurrence Relationships

Estimates of frequency-of-occurrence relationships begin with calculating a cumulative distribution function (cdf) for the response vector of interest, the maximum water-surface elevation. Let $X_1, X_2, X_3, ..., X_n$ be n identically distributed random-response variables with a cumulative cdf

$$F_X(x) = Pr[X \leq x] \tag{3}$$

where $Pr[\ ]$ represents the probability that the random variable X is less than or equal to some value x and $F_X(x)$ is the cumulative probability distribution function ranging from 0 to 1. The problem is to estimate the value of F_X without introducing some parametric relationship for computing the probability. The following procedure is adopted because it makes use of the probability laws defined by the data and does not incorporate any prior assumptions concerning the probability relationship.

Assume a set of n observations of data. The n values of x are first ranked in order of increasing size such that

$$x_{(1)} \leq x_{(2)} \leq x_{(3)} \leq \ldots \leq x_{(n)}$$

where the parentheses surrounding the subscript indicate that the data have been rank ordered. The value $x_{(1)}$ is the smallest in the series, and $x_{(n)}$ represents the largest. Let r denote the rank of the value $x_{(r)}$ such that rank 1 is the smallest and rank $r = n$ is the largest.

An empirical estimate of $F_X(x_{(r)})$, denoted by $\hat{F}_X(x_{(r)})$, is given by Gumbel (1954) (see also Borgman and Scheffner (1991) or Scheffner and Borgman (1992)).

$$\hat{F}_x(x_{(r)}) = \frac{r}{(n+1)} \tag{4}$$

for $\{x_{(r)}, r = 1, 2, 3, ..., n\}$. This form of estimate allows for future values of x to be less than the smallest observation $x_{(1)}$ with probability of $1/(n + 1)$ and to be larger than the largest value $x_{(n)}$ with probability $n/(n + 1)$. In the implementation of the EST, tail functions are used to define the cdf for events larger than the largest or smaller than the smallest observed event so that the cdf contains no discontinuity (Borgman and Scheffner 1991).

The estimated cdf as defined by Equation 4 is used to develop stage-frequency relationships in the following manner. Consider that the cdf for some storm response corresponding to an n-year return period event can be determined from:

$$F(x) = 1 - \frac{1}{n} \tag{5}$$

where $F(x)$ is the simulated cdf of the n-year impact. Frequency-of-occurrence relationships are obtained by linearly interpolating a stage from Equation 4 corresponding to the cfd associated with the return period specified in Equation 5.

Because multiple simulations are made, each yielding its own stage-frequency curve relationship, the average stage is computed for each return period year. Furthermore, for each return period, the standard deviation, defined as:

$$\sigma = \sqrt{\left[(1/N)\sum_{n=1}^{n=N}(x_n - \bar{x})\right]} \tag{6}$$

(where x bar is the mean value), is computed to define an error band of ± one standard deviation corresponding to the mean value for that particular return period year.

4 Description of Numerical Models

Generation of hurricane stage-frequency relationships for the study area can be divided into four interrelated tasks, each using a numerical model. In the first task, hurricane-induced wind and atmospheric pressure fields are generated to replicate those hurricanes that have impacted the study area. Using these wind and pressure fields, storm-surge events are simulated in the second task using a long-wave hydrodynamic model to obtain peak water-surface levels. These wind fields are also used in developing wave-setup levels with a wind-generated wave model in the third task. With the information obtained in the above tasks, the EST is employed, which utilizes the interrelationships of historic storm events and the computed maximum surge levels and wave setups. Application of the EST provides the desired stage-frequency relationships for the study area. Descriptions of the wind and atmospheric pressure model together with the hydrodynamic and wind-wave models are presented below.

Description of Wind and Atmospheric Pressure Field Model

The Planetary Boundary Layer (PBL) wind field model was selected for simulating hurricane-generated wind and atmospheric pressure fields. The model employs the vertically averaged primitive equations of motion for predicting wind velocities experienced within a hurricane. Through hindcast applications, Cardone, Greenwood, and Greenwood (1992) found that their model yields accurate surface wind speeds and directions when compared with measured data collected while the hurricane is in the open water. It is, therefore, the Coastal and Hydraulics Laboratory (CHL)-preferred model for generating tropical wind and atmospheric pressure fields.

Additionally, a moving coordinate system is defined such that its origin always coincides with the moving low-pressure center of the eye of the storm. Therefore, the standard equations of motion are transformed into the following relationships in Cartesian coordinates:

$$\frac{\partial u}{\partial t} + u\frac{\partial u}{\partial x} + v\frac{\partial u}{\partial y} - fv = \frac{1}{\rho}\frac{\partial p_c}{\partial x} + \frac{\partial}{\partial x}\left(K_H \frac{\partial u}{\partial x}\right) + \frac{\partial}{\partial y}\left(K_H \frac{\partial u}{\partial y}\right) + \frac{C_D}{h}|V|u \qquad (7)$$

$$\frac{\partial v}{\partial t} + u\frac{\partial v}{\partial x} + v\frac{\partial v}{\partial y} + fx = \frac{1}{\rho}\frac{\partial p_c}{\partial y} + \frac{\partial}{\partial x}\left(K_H \frac{\partial v}{\partial x}\right) + \frac{\partial}{\partial y}\left(K_H \frac{\partial v}{\partial y}\right) + \frac{C_D}{h}|V|v \qquad (8)$$

where

u and v = wind velocities in the x- and y-directions, respectively

ρ = mean air density

p_c = atmospheric pressure

K_H = horizontal eddy viscosity coefficient

C_D = drag coefficient

h = depth of the planetary boundary layer

V = magnitude of the wind velocity

The model includes parameterization of the momentum, heat, and moisture fluxes together with surface drag and roughness formulations.

An exponential pressure law is used to generate a circularly symmetric pressure field situated at the low-pressure center of the storm:

$$p_c(r) = p_0 + \Delta p e^{-(R/r)} \qquad (9)$$

where

p_0 = pressure at center or eye of storm

Δp (equal to $p - p_0$) = pressure anomaly with p taken as an average background or far-field pressure

R = scale radius, often assumed equivalent to radius to maximum wind

r = radial distance outward from the eye of storm

Wind speeds generated with the model are converted to surface wind stresses using the following relationship proposed by Garratt (1977):

$$\frac{\tau_x}{\rho_0} = C_D \frac{\rho_{air}}{\rho_0} |V| u \tag{10}$$

and

$$\frac{\tau_y}{\rho_0} = C_D \frac{\rho_{air}}{\rho_0} |V| v \tag{11}$$

where

τ_x and τ_y = wind stresses in the x- and y-directions, respectively

ratio ρ_{air}/ρ_0 = 0.001293 = ratio of air density to average density of seawater

C_D = frictional drag coefficient

The PBL hurricane wind model requires a series of "snapshots" for input consisting of a set of meteorological storm parameters defining the storm at various stages in its development or at particular times during its life. These parameters include latitude and longitude of the storm's eye, track direction and forward speed measured at the eye, radius to maximum winds, central and peripheral atmospheric pressures, and an estimate of the geostrophic wind speed and direction. Also, the direction and speed of steering currents can be provided for representing asymmetric hurricanes.

Some meteorological storm parameters were obtained from the hurricane database developed by the National Oceanic and Atmospheric Administration (NOAA)'s National Hurricane Center (NHC) (Jarvinen, Neumann, and Davis 1988). This database summarizes all hurricanes and tropical storms that occurred in the North Atlantic Ocean over the 104-year period from 1886 through 1989. Information contained in this database is provided at 0000, 0600, 1200, and 1800 hr Greenwich Mean Time (GMT) and includes latitude and longitude of the storm, central pressure, and maximum wind speed.

Radius to maximum winds is approximated using a function that incorporates the maximum wind speed and atmospheric pressure anomaly (Jelesnianski and Taylor 1973). Track directions and forward speeds required by the PBL model are approximated hourly, using cubic spline interpolation technique, from the storm's 6 hr latitudinal and longitudinal positions provided in the database. Peripheral atmospheric pressures were assumed equal to 1,013 mb, and geostrophic wind speeds were specified as 6 knots and have the same direction as the storm track.

The spatial area over which a hurricane resides is defined in the model via a numerical grid or a lattice network of nodes. Wind velocities and atmospheric pressures are computed at each node in the grid. Whereas some models employ a fixed grid system to simulate a hurricane (i.e., stationary grid with a moving storm), the PBL model simulates the hurricane as a stationary storm with a moving

grid. A hurricane's translational or forward motion is incorporated into model calculations by adding the forward and rotational velocity vector components.

The model uses a nested gridding technique, composed of five layers or subgrids, for computing the wind fields. Each subgrid measures 21 by 21 nodes in the x- and y-directions, respectively, and the centers of all subgrids, node (11,11), are defined at the eye of the hurricane. Whereas the number of nodes composing each subgrid is the same, the area of coverage and spatial resolution differs for each grid. For this study, the subgrid with the finest resolution had an incremental distance of 5 km between nodes. Incremental distances for the remaining subgrids were 10, 20, 40, and 80 km.

For each snapshot, the equations of motion are first solved using the grid covering the greatest area, which in this study is the grid having an incremental distance of 80 km between nodes. Computed wind velocities are then used as boundary conditions on the second-largest grid, and the equations of motion are solved again. This same procedure is followed for the remaining grids where wind fields are computed using sequentially smaller grids together with wind velocities computed with the next larger grid serving as boundary conditions. Thus, the nested gridding technique provides wind field information over a wide spatial area, while sufficient grid resolution is provided to accurately compute winds within the eye of the hurricane.

After all snapshots have been processed, hourly wind and atmospheric pressure fields are interpolated using a nonlinear blending algorithm that produces a smooth transition from one snapshot to the next. Hourly wind and pressure fields are then interpolated from the PBL grid onto the hydrodynamic grid and subsequently stored for use by the hydrodynamic model.

Description of Storm-Surge Model

The ADvanced CIRCulation (ADCIRC) numerical model was chosen for simulating the long-wave hydrodynamic processes in the study area. Imposing the wind and atmospheric pressure fields computed with the PBL model, the ADCIRC model can accurately replicate hurricane-induced storm-surge levels. The ADCIRC model was developed in the USACE Dredging Research Program (DRP) as a family of two- and three-dimensional finite element-based models (Luettich, Westerink, and Scheffner 1992; Westerink et al. 1992). Model attributes include the following capabilities:

a. Simulating tidal circulation and storm-surge propagation over very large computational domains while simultaneously providing high resolution in areas of complex shoreline configuration and bathymetry. The targeted areas of interest included continental shelves, nearshore areas, and estuaries.

b. Representing properly all pertinent physics of the three-dimensional equations of motion. These include tidal potential, Coriolis, and all nonlinear terms of the governing equations.

c. Providing accurate and efficient computations over time periods ranging from months to years.

In two dimensions, the model is formulated using the depth-averaged shallow water equations for conservation of mass and momentum. Furthermore, the formulation assumes that the water is incompressible, that hydrostatic pressure conditions exist, and that the Boussinesq approximation is valid. Using the standard quadratic parameterization for bottom stress and neglecting baroclinic terms and lateral diffusion/dispersion effects, the following set of conservation equations in primitive, nonconservative form, and expressed in a spherical coordinate system, are incorporated in the model (Flather 1988; Kolar et al. 1993):

$$\frac{\partial U}{\partial t}+\frac{1}{r\cos\phi}U\frac{\partial U}{\partial \lambda}+\frac{1}{R}V\frac{\partial U}{\partial \phi}-\left[\frac{\tan\phi}{R}U+f\right]V=$$

$$-\frac{1}{R\cos\phi}\frac{\partial}{\partial \lambda}\left[\frac{p_s}{\rho_0}+g(\zeta-\eta)\right]+\frac{\tau_{s\lambda}}{\rho_0 H}-\tau_* U \tag{12}$$

$$\frac{\partial V}{\partial t}+\frac{1}{r\cos\phi}U\frac{\partial V}{\partial \lambda}+\frac{1}{R}V\frac{\partial V}{\partial \phi}-\left[\frac{\tan\phi}{R}U+f\right]U= \tag{13}$$

$$-\frac{1}{R}\frac{\partial}{\partial \phi}\left[\frac{p_s}{\rho_0}+g(\zeta-\eta)\right]+\frac{\tau_{s\lambda}}{\rho_0 H}-\tau_* V$$

$$\frac{\partial \zeta}{\partial t}+\frac{1}{R\cos\phi}\left[\frac{\partial UH}{\partial \lambda}+\frac{\partial (UV\cos\phi}{\partial \phi}\right] \tag{14}$$

where

t = time

λ and φ = degrees longitude (east of Greenwich is taken positive) and degrees latitude (north of the equator is taken positive)

ζ = free surface elevation relative to the geoid

U and V = depth-averaged horizontal velocities in the longitudinal and latitudinal directions, respectively

R = the radius of the Earth

$H = \zeta + h$ = total water column depth

h = bathymetric depth relative to the geoid

$f = 2\Omega \sin \varphi$ = Coriolis parameter

Ω = angular speed of the Earth

p_s = atmospheric pressure at free surface

g = acceleration due to gravity

η = effective Newtonian equilibrium tide-generating potential parameter

ρ_0 = reference density of water

$\tau_{s\lambda}$ and $\tau_{s\varphi}$ = applied free surface stresses in the longitudinal and latitudinal directions, respectively

τ = bottom shear stress and is given by the expression $C_f(U^2 + V^2)^{1/2}/H$ where C_f = the bottom friction coefficient

The momentum equations (Equations 12 and 13) are differentiated with respect to λ and τ and substituted into the time differentiated continuity equation (Equation 14) to develop the following Generalized Wave Continuity Equation (GWCE):

$$\frac{\partial^2 \zeta}{\partial t^2} + \tau_0 \frac{\partial \zeta}{\partial t} - \frac{1}{R\cos\phi}\frac{\partial}{\partial \lambda}\left[\frac{1}{R\cos\phi}\left(\frac{\partial HUU}{\partial \lambda} + \frac{\partial (HUV\cos\phi)}{\partial \phi}\right) - UVH\frac{\tan\phi}{R}\right]$$

$$\left[-2\omega\sin\phi\, HV + \frac{H}{R\cos\phi}\frac{\partial}{\partial \lambda}\left(g(\zeta - \alpha\eta) + \frac{p_5}{\rho}p_0\right) + \tau^* HU - \tau_0 HU - \tau_{s\lambda}\right]$$

$$-\frac{1}{R}\frac{\partial}{\partial \phi}\left[\frac{1}{R\cos\phi}\left(\frac{\partial HVV}{\partial \lambda} + \frac{\partial HVV\cos\phi}{\partial \phi}\right) + UUH\frac{\tan\phi}{R} + 2\omega\sin\phi\, HU\right] \quad (15)$$

$$+\frac{H}{R}\frac{\partial}{\partial \phi}\left(g(\zeta - alfa\eta) + \frac{p_s}{\rho_0}\right) + \tau^* - \tau_0 HV - \frac{\tau_{s\lambda}}{\rho_0}]$$

$$-\frac{\partial}{\partial t}[\frac{VH}{R}\tan\phi] - \tau_0[\frac{VH}{R}\tan\phi] = 0$$

The ADCIRC-2DDI model solves the GWCE in conjunction with the primitive momentum equations given in Equations 12 and 13. The GWCE-based solution scheme eliminates several problems associated with finite-element

programs that solve the primitive forms of the continuity and momentum equations, including spurious modes of oscillation and artificial damping of the tidal signal. Forcing functions include time-varying water-surface elevations, wind shear stresses, atmospheric pressure gradients, and the Coriolis effect. Also, the study area can be described in ADCIRC using either a Cartesian (i.e., flat earth) or spherical coordinate system.

The ADCIRC model uses a finite-element algorithm in solving the defined governing equations over complicated bathymetry encompassed by irregular sea/shore boundaries. This algorithm allows for extremely flexible spatial discretizations over the entire computational domain and has demonstrated excellent stability characteristics. The advantage of this flexibility in developing a computational grid is that larger elements can be used in open-ocean regions where less resolution is needed, whereas smaller elements can be applied in the nearshore and estuary areas where finer resolution is required to resolve hydrodynamic details.

Figure 2 shows the numerical grid used by ADCIRC in the present study. The grid covers the entire western North Atlantic Ocean including the Gulf of Mexico and Caribbean Sea. The domain is bounded to the east at 60 deg west longitude and landward by the east coast of North, Central, and South America in the Northern Hemisphere. Figure 3 shows an enlarged portion of the grid near Wilmington, NC. Figure 4 shows grid refinement in the vicinity of the BNP site that includes high resolution in the project area and extends offshore from the coast to the 50-ft contour line, and in the lower reach of Cape Fear River from Wilmington, NC, to the Atlantic Ocean. Small elements were used to resolve the complicated bathymetry and irregular land-water boundary geometry in the study area. Figure 5 shows the nearshore and offshore bottom contours near the BNP site. The high-resolution grid in the BNP site and its surrounding area requires detailed bathymetric and topographic data for land and nearshore bottom elevation information. This information was obtained from three sources: (a) U.S. Defense Mapping Agency charts; (b) NOAA National Ocean Survey/Coast and Geodetic Survey charts; and (c) U.S. Army Map Service charts.

Description of Wave Model

The Wave Information Studies WAVE (WISWAVE) model is a second-generation discrete directional spectral wave model where the spectral wave-height computations are based on integration of energy over the discrete frequency spectrum. It uses a finite-difference computational scheme to simulate generation, dissipation, and propagation of water waves via winds and wave interactions. Model output includes time-series of significant wave height, peak (dominant) or mean wave period, and mean wave direction. Peak or dominant wave periods are not integrated quantities in that they are not derived by summation over the spectrum. Peak period is defined as the period associated with the midband frequency of that frequency band containing the largest spectral energy density. Mean wave period, as calculated by the model, is an energy-weighted quantity integrated over all user-specified frequencies of interest. Model input includes a computational grid, with corresponding water depths at each node in the grid, wind speeds and

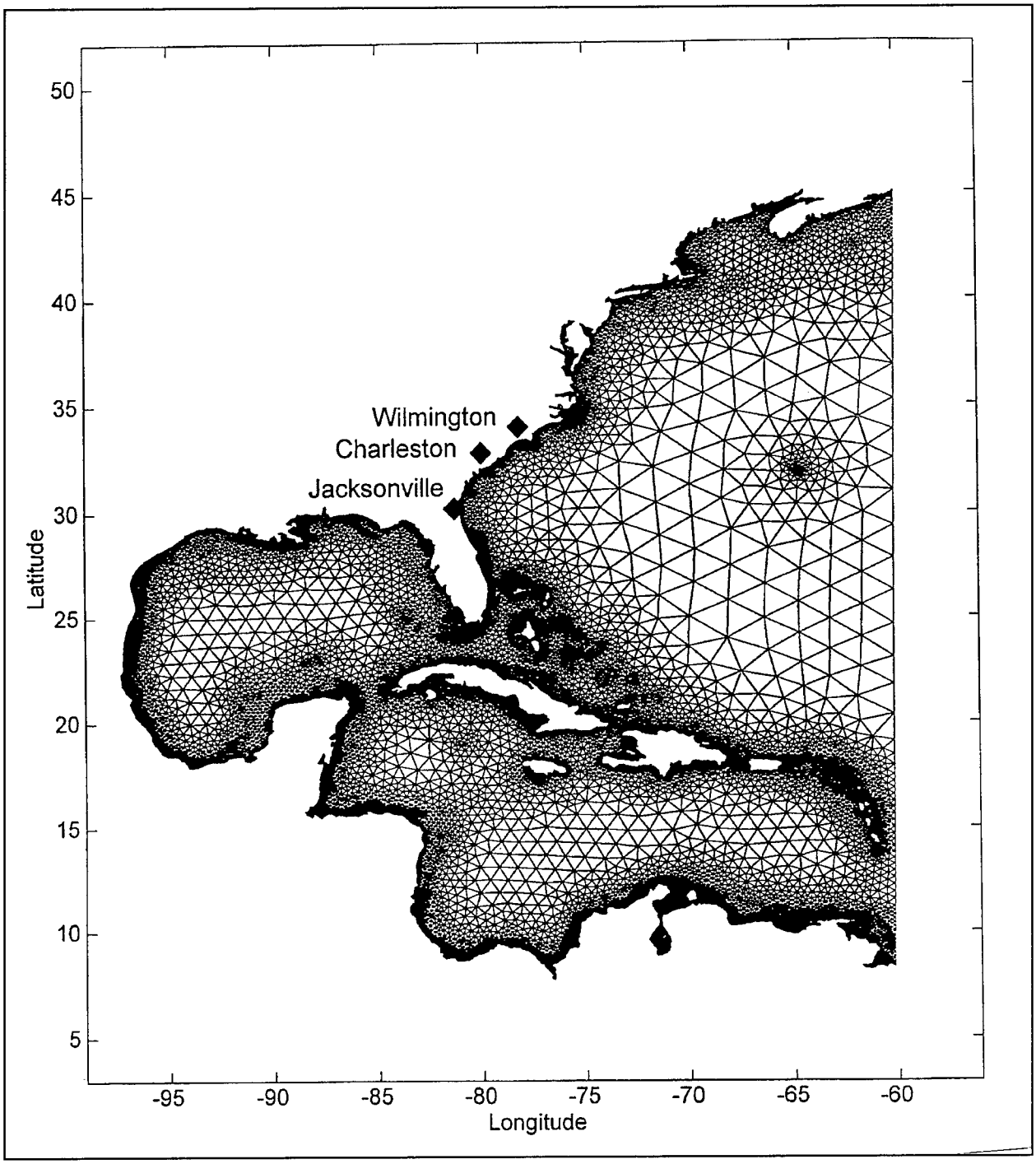

Figure 2. Finite-element grid used in the ADCIRC computation of storm surges

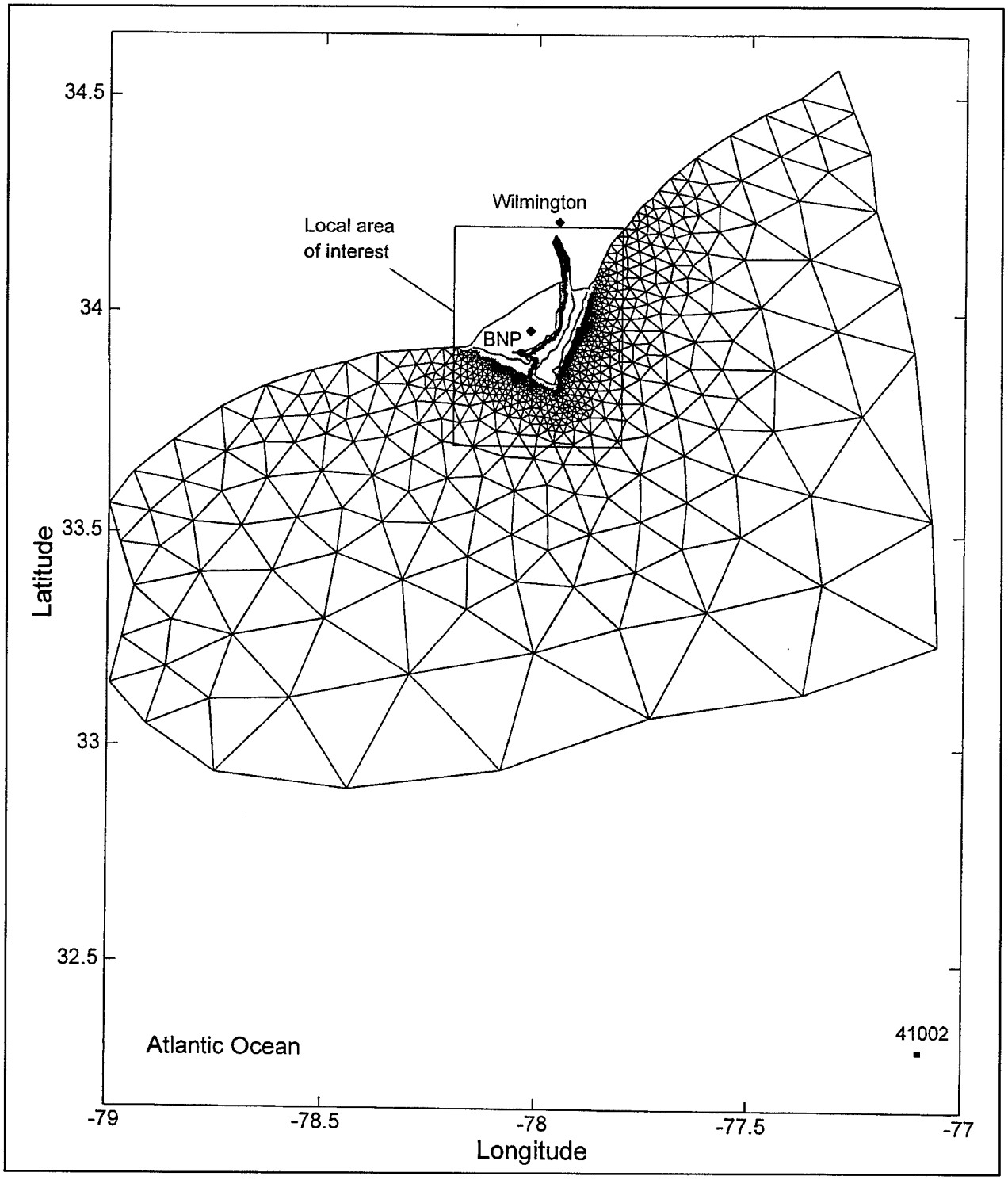

Figure 3. Detail of finite-element grid near Wilmington, NC

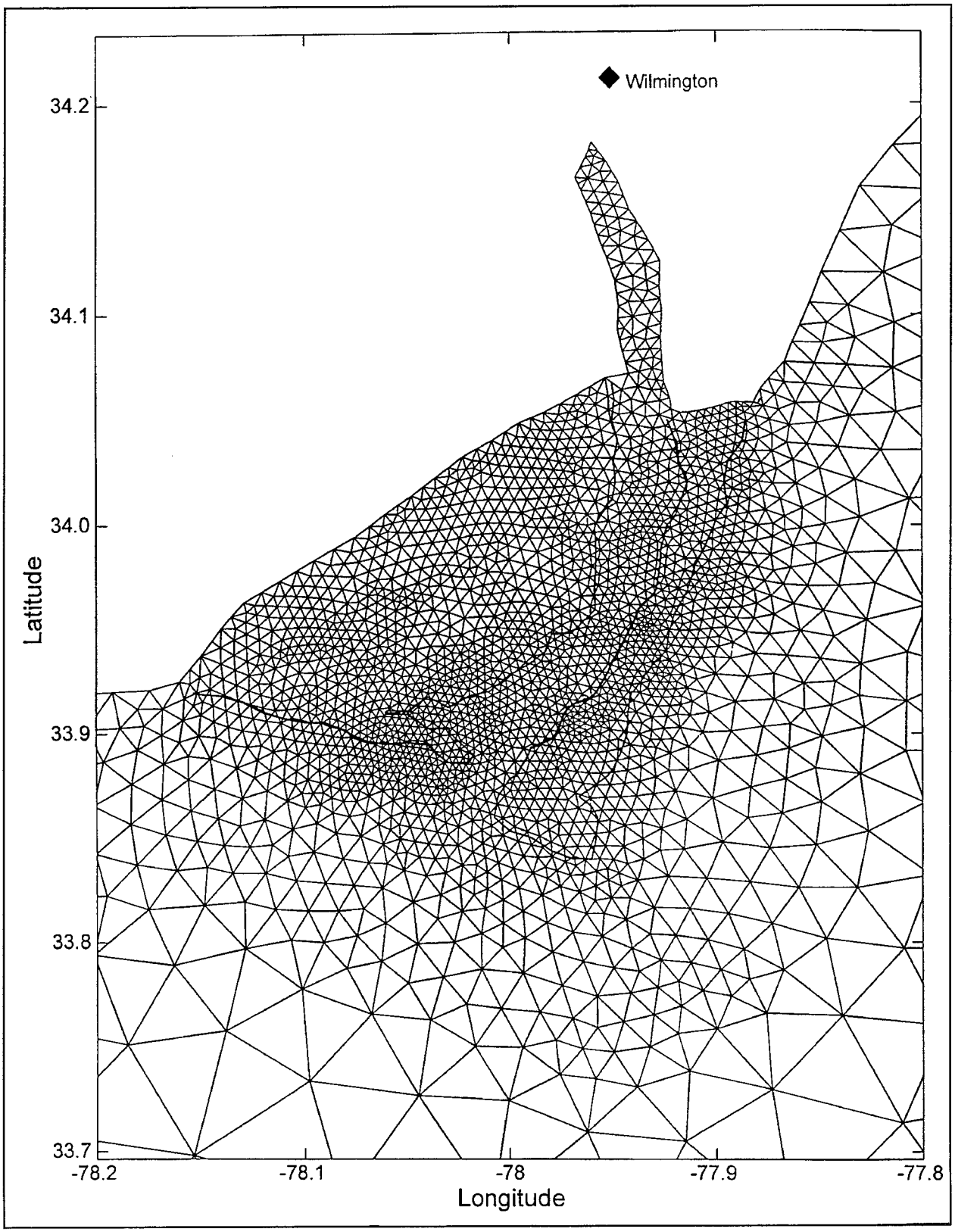

Figure 4. Detail of refined subgrid in the vicinity of the BNP site

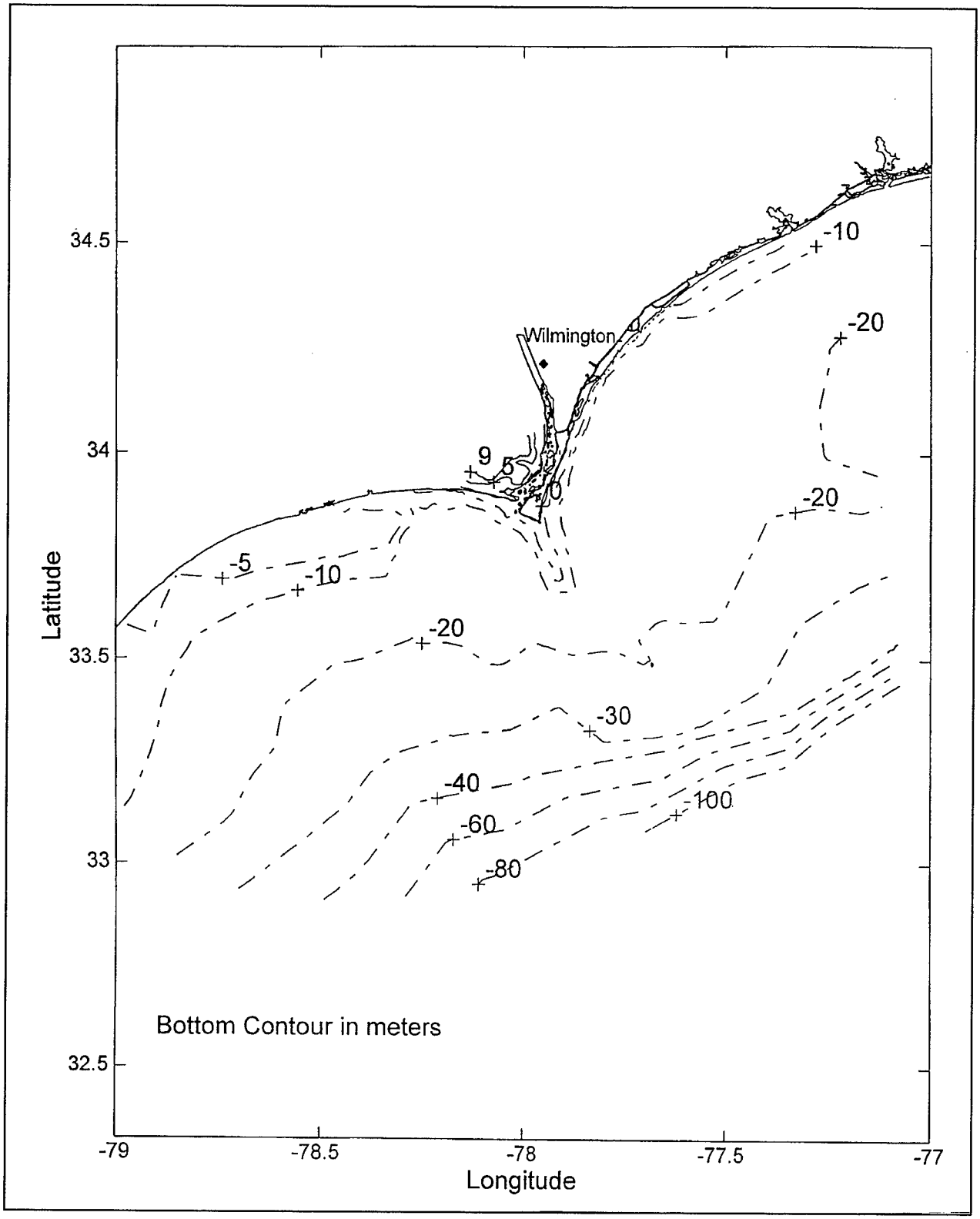

Figure 5. Nearshore and offshore bathymetry near the BNP site

directions over the entire modeling domain, and wave conditions along the outer boundary of the grid.

Wave modeling was conducted using a nested grid approach where wave conditions were computed using three distinct grids. Each grid had a different spatial resolution and coverage area. The coarser grid, referred to as Level 1, covers nearly the entire North Atlantic Ocean and has a nodal spacing or resolution of 1 deg in latitude and longitude. The next finer grid, referred to as Level 2, covers the continental shelf area east of the U.S. Atlantic coastline and has a resolution of 0.25 deg. Figure 6 shows the computational domains of Levels 1 and 2.

Using the wind fields produced with the PBL model, wave conditions are computed first on the coarse-resolution grid. Time-series of wave heights and periods are saved at those nodes coinciding with the boundary nodes of the Level 2 grid. These time-series serve as boundary conditions for wave conditions computed using the Level 2 model.

This same procedure is followed again with the Level 2 model where wave conditions are computed using the PBL-generated wind fields and time-series of wave heights and periods are subsequently saved. These time-series are saved at locations in close proximity of the BNP site and serve as boundary conditions for the finest resolution grid, referred to as the Level 3 grid.

The Level 3 grid is necessary in order to accurately depict the shallow-water effects, such as shoaling, refraction, breaking, and wave setup in the vicinity of the BNP. A simple time-dependent, wave-transformation model is used for this purpose. The shallow-water model is run in a rather small domain, which is shown as Level 3 in Figure 5. The model does not include the surface wind input under the assumption that energy exchange between winds and waves is negligible because of the small water body encompassed by Level 3. Unlike WISWAVE, which runs on a latitude-longitude parallel grid, the shallow-water model uses an unstructured grid that is identical to the grid system shown in Figures 2, 3, and 4.

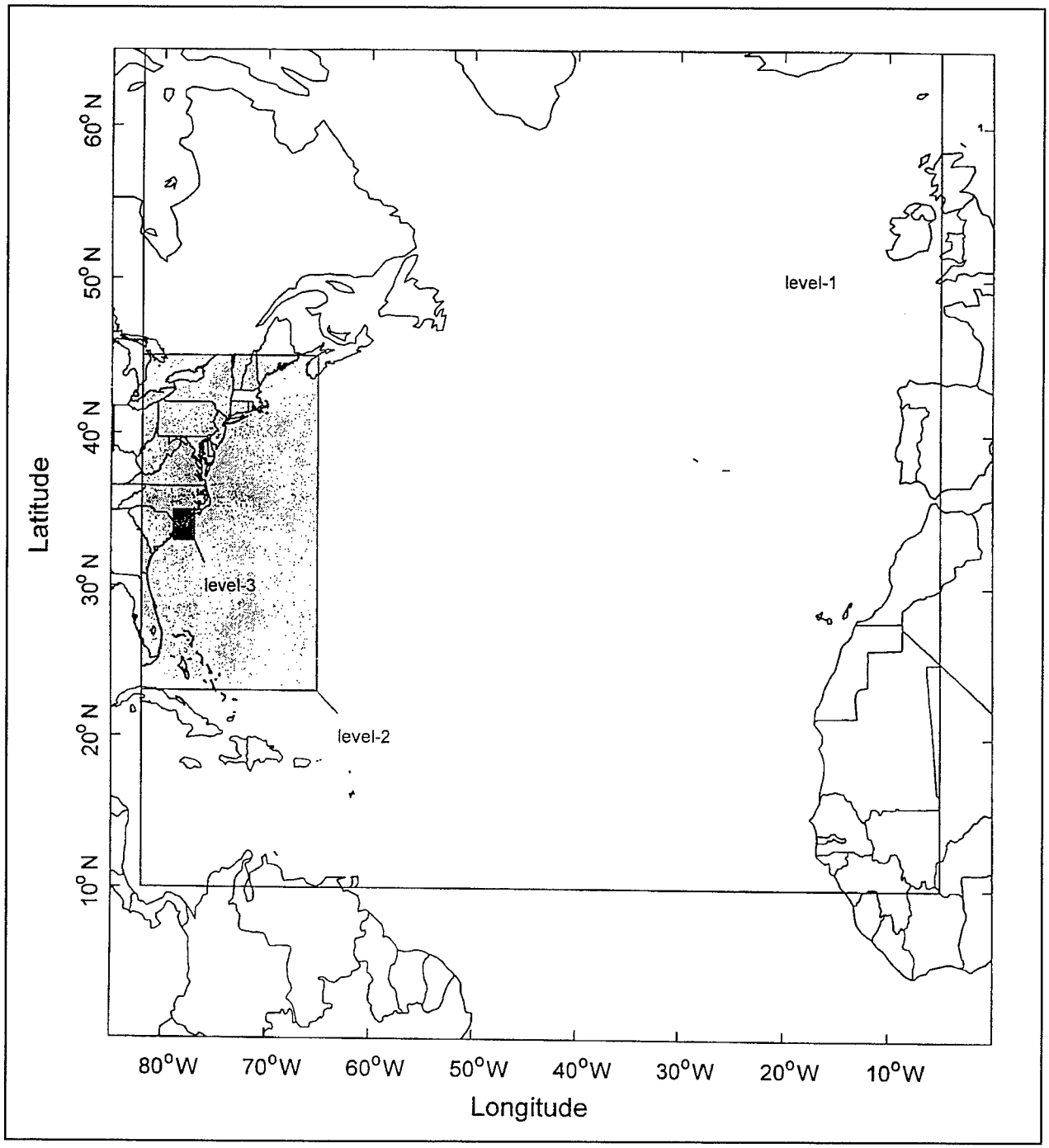

Figure 6. Computational domains for WISWAVE simulation of storm waves

5 Implementation of Numerical Models

During construction of a numerical model, the model must undergo validation exercises to ensure that it accurately predicts hydrodynamic conditions within the study area. Accuracy of model results is greatly influenced by the accuracy of boundary and forcing conditions, representation of the geometry of the study area (i.e., bathymetry and land/water interface), and to a lesser degree, the choice of certain parameters, such as the bottom friction coefficient. Validation exercises were conducted for both the storm surge and wave models via hindcast simulations of Hurricane Hugo, which impacted the study area in September 1989.

Validation of Storm-Surge Model

The hindcast simulation began on 10 September 1989 at 0600 GMT and ended on 21 September at 1200 GMT. A 30-sec time-step was used in the simulation. Wind and atmospheric pressure fields were computed using the PBL model, and tidal forcing was specified at the open-water boundary. Tidal elevations imposed at the open-water boundary were synthesized using the M_2, S_2, N_2, K_1, O_1, P_1, Q_1, and K_2 constituents.

From the beginning of the simulation to 17 September at 0000 GMT, no wind or atmospheric pressures were included in the model. This 7-day period provided sufficient simulation time to develop an accurate tidal current field and to dampen any start-up errors. Thereafter, wind and atmospheric pressure fields were supplied to the model at hourly increments. These fields were computed independently of adjacent weather systems (e.g., high-pressure cells) using a constant far-field atmospheric pressure of 1,013 mb. In addition, nodal wind and pressure values were linearly interpolated at time-steps falling between whole hours.

Figure 7 shows a snapshot of wind fields generated by the PBL model for Hurricane Hugo before landfall on the South Carolina coast. Figure 8 presents a comparison of model-generated and measured water-surface elevations recorded at Charleston, South Carolina (Cooper River entrance), for the period of 21 September at 0000 GMT through 0000 GMT on 24 September. Comparison between the computed and measured surge data shows good agreement.

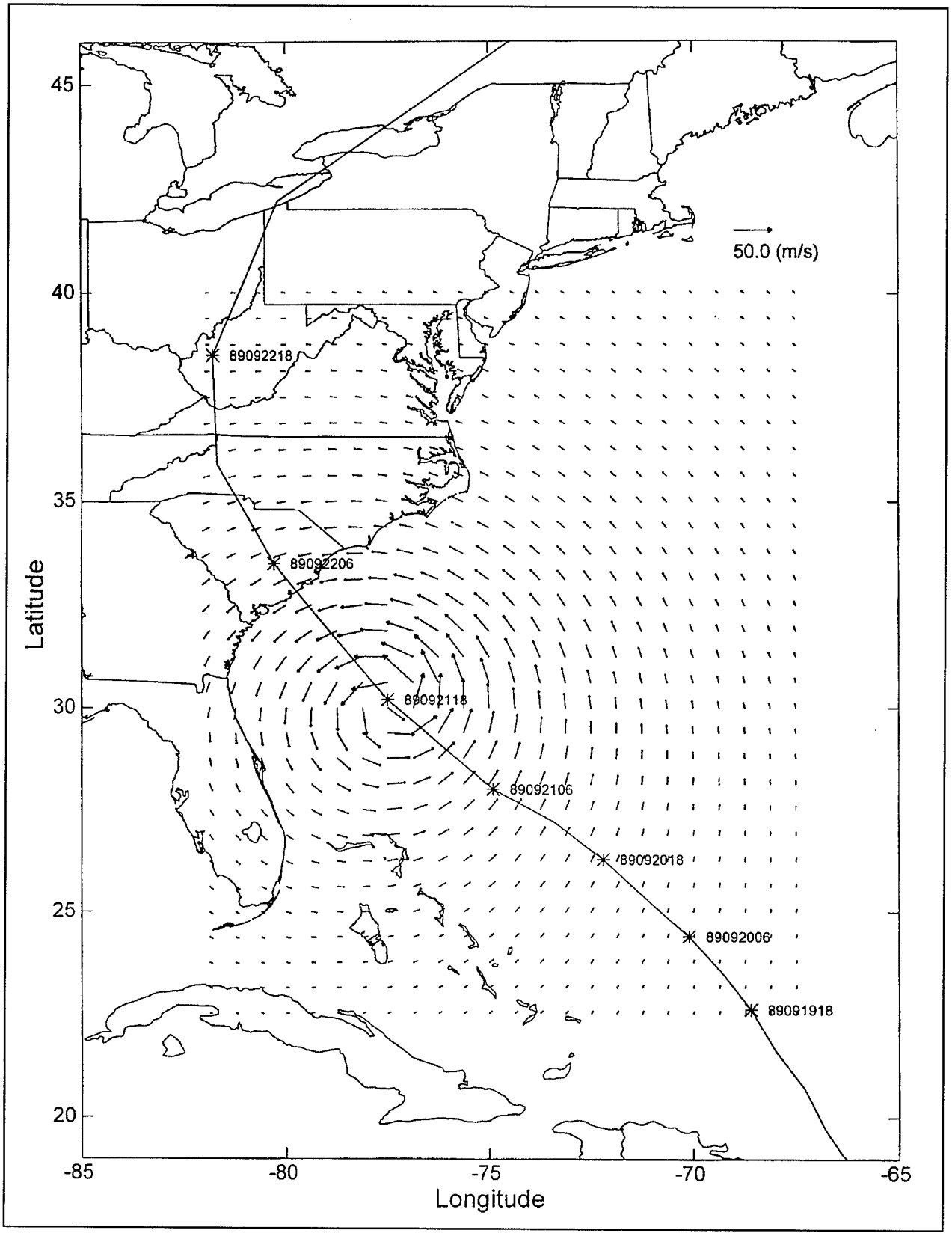

Figure 7. Computer-generated wind field for Hugo

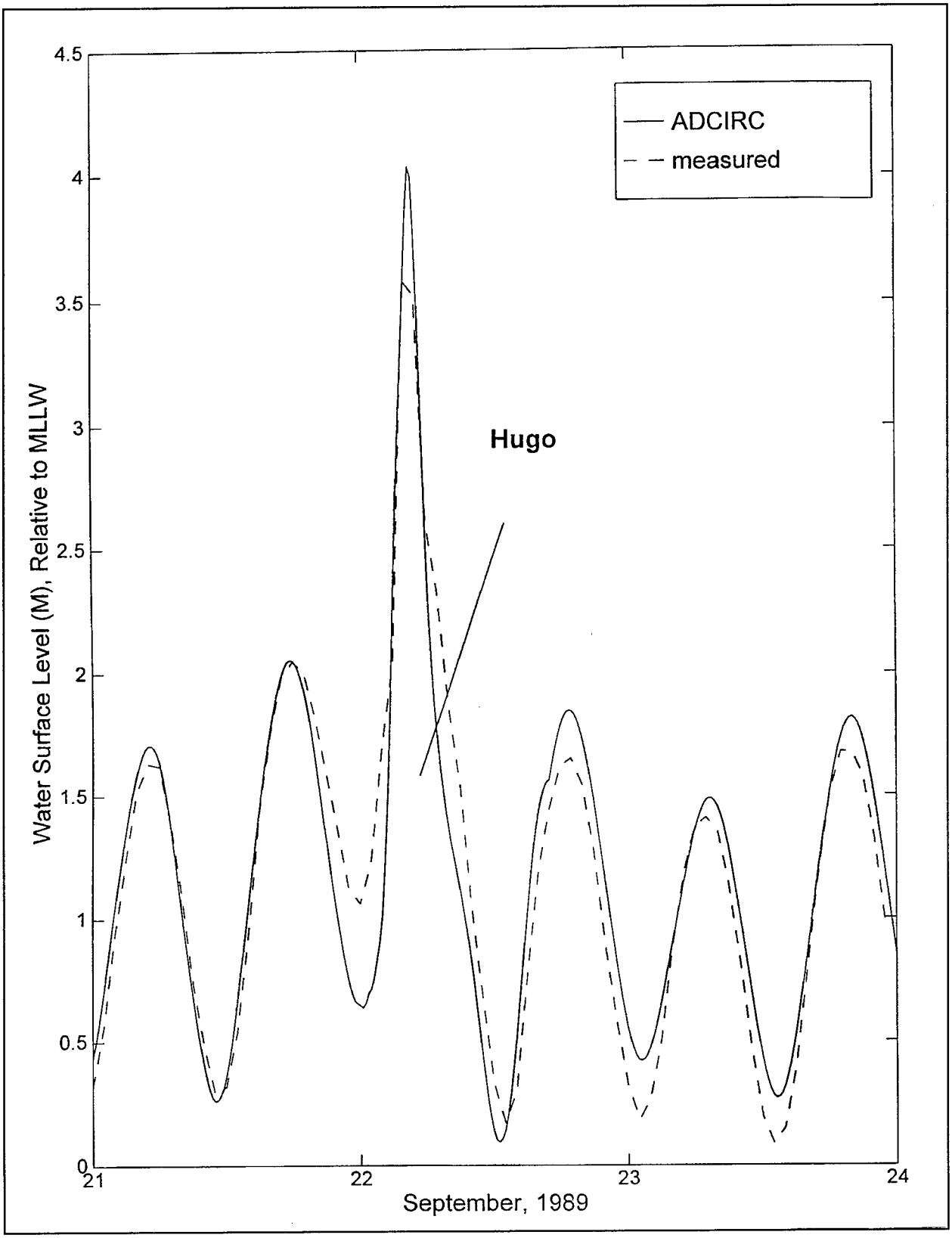

Figure 8. Comparison of computed and measured water-level elevations

Figure 9 presents the storm-surge distribution in the vicinity of the BNP area during landfall of Hurricane Hugo. Because the hurricane made landfall about 100 km southwest of the BNP site, the maximum surge at the BNP site is relatively small compared with the Charleston area. In Figures 10 and 11, the storm-surge computation for Hurricane Hugo included the astronomical tides in order to facilitate comparison with measured data.

Validation of Wave Model

Waves induced by Hurricane Hugo were simulated using the nested wave models. Wind fields supplied to the wave models were computed using the PBL model; however, adjacent weather systems were included in the wind fields by inserting wind velocities produced by the National Center of Environmental Prediction (NCEP) at all nodes lying beyond the periphery of the hurricane.

Wave conditions were first hindcasted using the coarse resolution (i.e., Level 1). Time-series of wave heights and periods were stored at those nodes, on the Level 1 grid, that coincide with the boundary nodes of the Level 2 grid. Using these data as boundary conditions, the hurricane was then simulated with the Level 2 model, saving time-series of wave heights and periods at those nodes coinciding with the boundary nodes on the Level 3 grid. Lastly, wave conditions were computed with the Level 3 model, which has sufficient resolution (where the other grids do not) for depicting shoaling, refraction, breaking, etc. Wind fields were incorporated into the Level 1 and 2 simulations, but not in the Level 3 simulation.

Figure 10 provides a comparison of computed and measured wave heights for Hurricane Hugo. The buoy that measured these heights is located at approximately 75 deg west longitude, 31 deg north latitude, or about 4 deg east of the South Carolina coast. Figure 11 displays the computed wave-height distribution, using the Level 3 grid, induced by Hurricane Hugo.

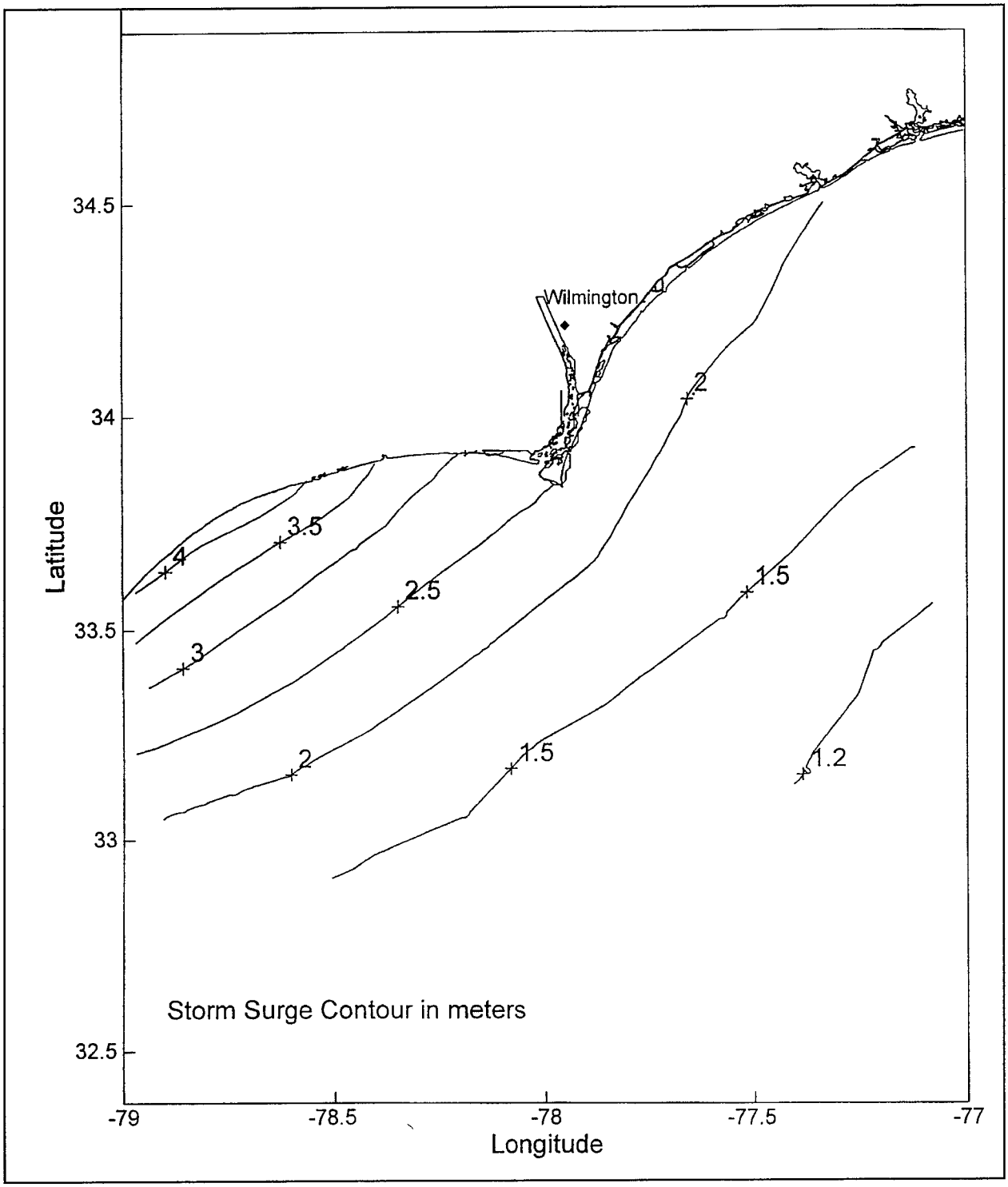

Figure 9. ADCIRC result of water-level elevation contours for Hugo

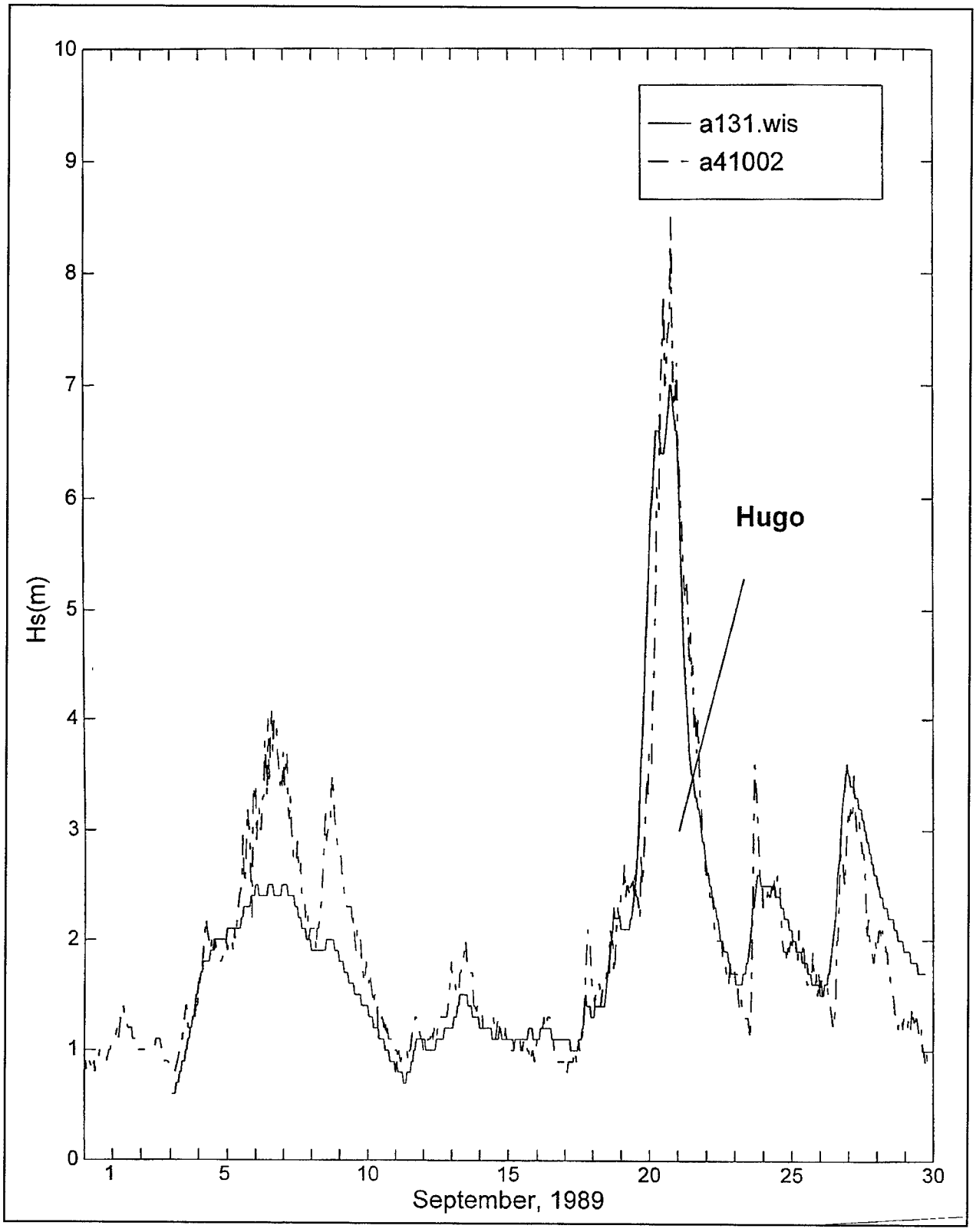

Figure 10. Comparison of computed and measured waves for Hugo

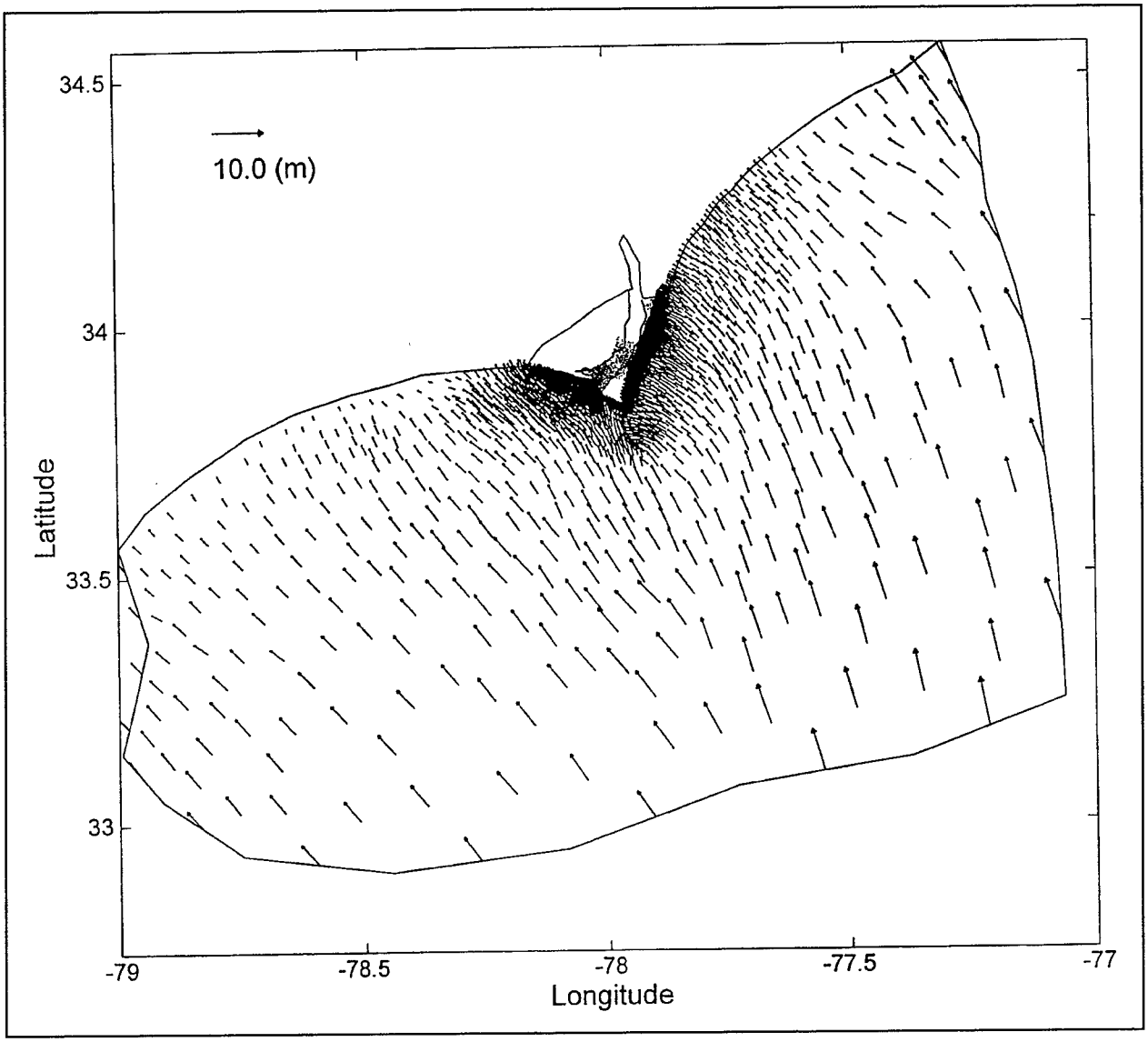

Figure 11. Computer-simulated wave-height distribution for Hugo

6 Development of Stage-Frequency Relationships

The process of generating stage-frequency relationships for the BNP site consisted of four sequential tasks. First, a set of historical hurricanes that impacted the study area were selected, and the PBL wind field model was used to replicate the wind and atmospheric pressure fields generated by these storms. Second, using the output generated by the PBL model, storm-surge elevations were computed using the ADCIRC model. Time-series of storm-surge elevations were stored at numerous locations along the study reach at which stage-frequency relationships were desired. Third, the nested wave models were used in simulating wind-generated waves using the PBL-generated winds. Fourth, with the descriptive parameters defining the simulated hurricane events, together with resulting storm-surge elevations and wave heights, the EST was employed to compute the stage-frequency relationships. A description of the methodology used in performing these tasks is presented below.

Selection of Hurricanes

Because stage-frequency relationships are based on a statistical analysis of storm-surge elevations resulting from historical storm events, a thorough analysis is required to define all tropical storm events that have impacted the study area. To perform this task, the Tropical Event Database-Surge (TEDS), developed through the USACE DRP (Scheffner et al. 1994), was used.

TEDS contains peak surge elevations for 134 historical tropical storms at 484 shoreline locations along the east and Gulf of Mexico coasts of the United States. Peak surge elevations were computed using the ADCIRC model, and meteorological storm parameters were obtained from the NHC database, which summarizes all hurricanes and tropical storms that occurred in the North Atlantic Ocean over the 104-year period from 1886 through 1989. The NHC database contains storm parameters for 875 tropical storms and depressions. (All storms that failed to induce a minimum 1-ft surge at any of the 484 stations were omitted from TEDS, which is why TEDS contains surges from only 134 events.)

For this analysis, all tropical storms and hurricanes that affected the Mid-Atlantic States were selected for the training set. These include all hurricane and

tropical storm events occurring since the development of the TEDS. This procedure identified 24 events, and these events are presented in Table 1. Figure 12 shows the storm tracks of each event.

Table 1
List of 24 Tropical Events Selected for Storm-Surge Study

Case Number	Year/Month	Name	HURDAT Identification Number	Max. Wind knot	Minimum Center Pressure mb
1	1996 / Sep.	Fran	944	105	946
2	1996 / July	Bertha	940	100	960
3	1989 / Sep.	Hugo	872	140	918
4	1985 / Nov.	Kate	839	105	954
5	1984 / Sep.	Diana	820	115	949
6	1982 / June		807	60	984
7	1981 / Aug.	Dennis	797	65	995
8	1972 / June	Agnes	712	75	977
9	1968 / Oct.	Gladys	669	75	965
10	1964 / Sep.	Dora	630	100	964
11	1960 / Sep.	Donna	597	140	932
12	1959 / Sep.	Gracie	589	120	950
13	1956 / Sep.	Flossy	562	80	980
14	1954 / Oct.	Hazel	541	120	937
15	1953 / Sep.	Florence	526	110	968
16	1947 / Oct.		465	75	973
17	1944 / Oct.		440	105	968
18	1944 / Aug.		432	80	990
19	1935 / Sep.		353	140	892
20	1930 / Sep.		299	130	933
21	1929 / Oct.		296	120	936
22	1928 / Sep.		292	140	929
23	1916 / July		217	85	983
24	1910 / Oct.		194	105	941

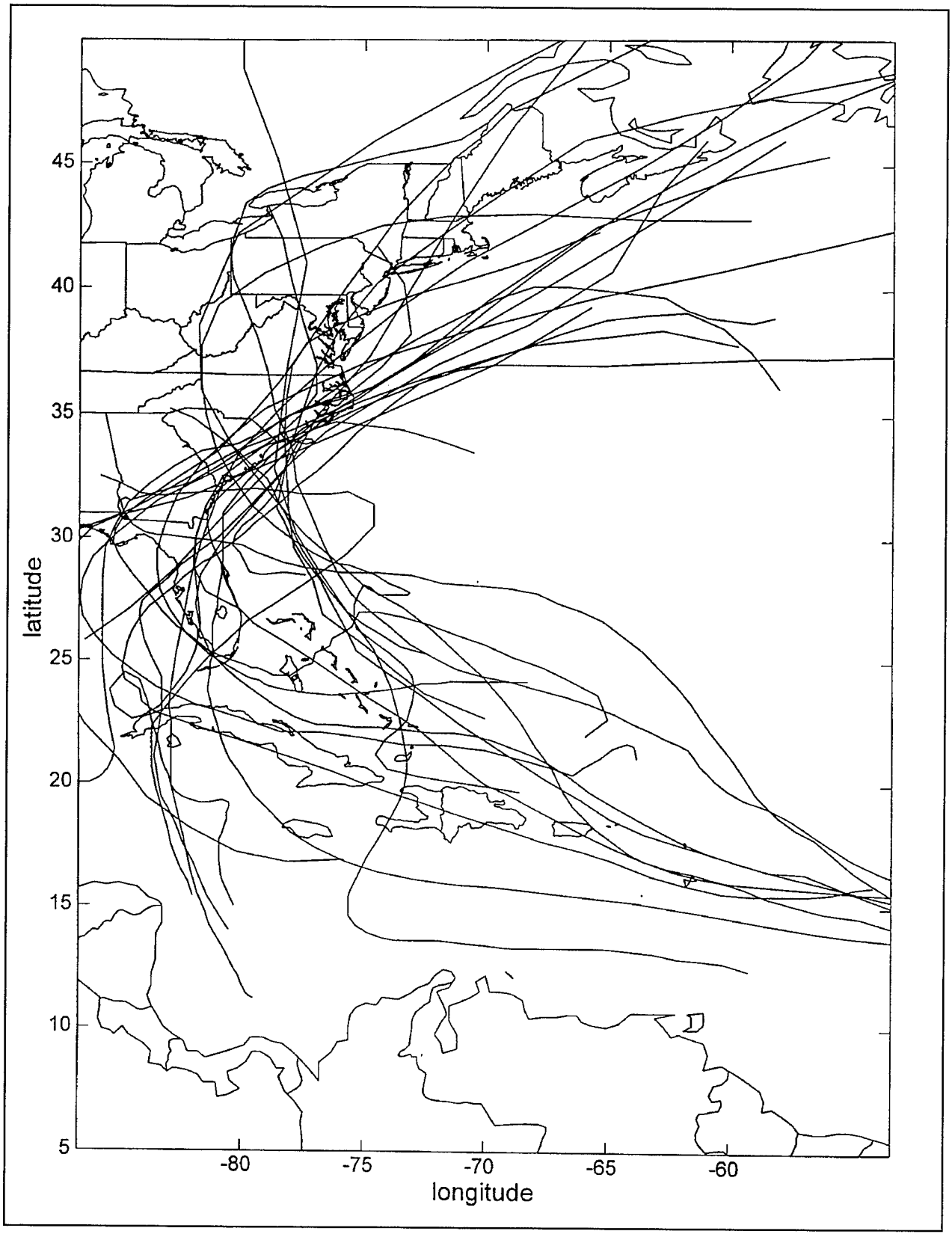

Figure 12. Tropical storm tracks impacting the BNP site

In order to create the worst (realistic) hurricane for the BNP site, two hypothetical events were synthesized using Hurricane Hugo, which had the lowest pressure deficit of any historical storm that affected the study area. One hypothetical event was created by shifting the track of Hurricane Hugo northeast by 1.4 deg, whereas the second event had a track that was 1.4 deg southwest of the historical track. All other storm parameters for these hypothetical storms were set equal to those measured for Hurricane Hugo.

Together with the 24 historical events and two hypothetical events, the training set used in the EST contained 26 storms. Each event was then simulated using the PBL, ADCIRC, and WISWAVE models to compute the wind and atmospheric pressure fields, storm-surge elevations, and wave conditions, respectively, at 12 stations located within the study area (Table 2, Figure 13).

Application of Storm-Surge Model

All 26 storms presented in Table 2, which includes both the historical and hypothetical hurricanes, were simulated with the storm-surge model. Starting and ending times of each storm simulation corresponds to the first and last entry contained in the NHC database for that particular storm. Furthermore, each storm-surge simulation began with the hurricane residing at its initial position listed in the database and concluded at its ending position. Thus, each simulation began when the hurricane was far away from the study area. For all hurricanes, a temporal "ramp" was used to slowly increase, over a 1-day period, wind stresses and pressure gradients from zero to their measured intensity. Using this ramp eliminates spurious modes of oscillation caused by suddenly imposing full-force winds and pressure gradients on the flow field.

All storm-surge simulations were performed independently of tidal action, eliminating the task of extracting surge levels from a time-series of combined tide- and surge-induced water-surface elevations. Therefore, storm-surge elevations computed in this task can be considered as approximations of the historical events. Although the frequencies associated with their maximum surge may be considered relatively accurate, the value of the peak surge may not correspond to historically observed surge elevations. The hydrographs should therefore not be considered hindcast of the historical events for the following two reasons. First, the storm events were simulated without tides; therefore, peak values do not reflect the tidal stage at the time of their occurrence.

Second, the hurricane parameters estimated from the storm database are only approximate; all information necessary to numerically simulate each event is unknown and has not been calibrated. For example, values of central pressure, radius to maximum winds, and far-field pressure are not known and were estimated from available data or observations. Because little data exist for the earlier storms, a consistent approach for selecting storm parameters was developed. This approach may not produce an accurate surge elevation for a particular event; however, it is felt that the final full population of storm data from which storm statistics are computed is representative of the range of historical events and should produce reliable and accurate hurricane stage-frequency relationships.

Table 2
Maximum Storm-Surge Elevation (m) Based on ADCIRC Simulations

	Station											
Case	1	2	3	4	5	6	7	8	9	10	11	12
1	1.51	1.34	1.37	1.73	2.07	2.08	0.78	0.75	0.67	2.21	2.14	2.13
2	1.64	1.63	1.71	2.08	2.17	1.85	0.79	0.70	0.65	1.25	1.31	1.40
3	1.94	1.91	1.96	1.78	1.89	1.99	1.78	1.83	1.94	1.31	1.30	1.29
4	1.71	1.82	1.52	1.66	1.54	1.53	1.18	1.22	1.18	0.37	0.40	0.43
5	1.79	1.96	1.88	1.92	1.78	1.58	0.45	0.47	0.51	1.66	1.56	1.59
6	0.38	0.37	0.37	0.36	0.28	0.20	0.42	0.40	0.40	0.44	0.51	0.63
7	0.60	0.72	0.60	0.60	0.55	0.56	0.67	0.73	0.70	0.28	0.27	0.28
8	1.76	1.77	1.48	1.95	2.23	2.09	0.52	0.58	0.57	0.12	0.17	0.21
9	0.21	0.23	0.21	0.18	0.19	0.20	0.23	0.24	0.24	0.39	0.38	0.39
10	0.77	0.66	0.71	0.79	0.88	1.03	0.61	0.67	0.65	0.19	0.19	0.24
11	0.13	0.00	0.13	0.11	0.11	0.13	0.19	0.16	0.18	1.40	1.39	1.35
12	0.81	0.83	0.80	0.83	0.89	0.97	0.77	0.84	0.86	0.60	0.63	0.67
13	1.04	0.86	0.87	1.23	1.47	1.66	0.75	0.83	0.83	0.28	0.33	0.37
14	3.25	3.34	3.33	2.94	2.62	2.56	2.99	3.21	3.26	2.20	2.22	2.26
15	0.57	0.77	0.63	0.50	0.40	0.31	0.79	0.83	0.85	0.82	0.82	0.82
16	0.25	0.23	0.26	0.23	0.22	0.22	0.28	0.30	0.31	0.46	0.45	0.45
17	0.59	0.59	0.55	0.63	0.68	0.79	0.48	0.53	0.53	0.17	0.19	0.22
18	0.76	0.79	0.74	0.67	0.50	0.60	0.72	0.84	0.85	0.56	0.55	0.58
19	1.83	1.76	1.73	2.01	2.22	2.47	1.48	1.63	1.65	0.83	0.93	0.97
20	0.26	0.00	0.29	0.22	0.21	0.21	0.35	0.36	0.38	0.62	0.59	0.58
21	0.67	0.63	0.63	0.74	0.85	0.99	0.54	0.60	0.61	0.26	0.29	0.32
22	2.08	1.92	1.88	2.08	2.17	2.48	1.55	1.61	1.65	0.68	0.81	1.06
23	0.29	0.32	0.30	0.28	0.29	0.32	0.31	0.34	0.36	0.24	0.24	0.25
24	1.79	1.85	1.57	2.02	2.25	2.38	1.55	1.64	1.60	1.17	1.28	1.43
25[a]	2.84	2.96	2.97	2.76	2.69	2.93	2.43	2.63	2.70	2.38	2.40	2.45
26[a]	0.78	0.83	0.80	0.72	0.71	0.78	0.83	0.90	0.92	0.83	0.82	0.83

[a] Hypothetical events representing shifting of Hurricane Hugo track.

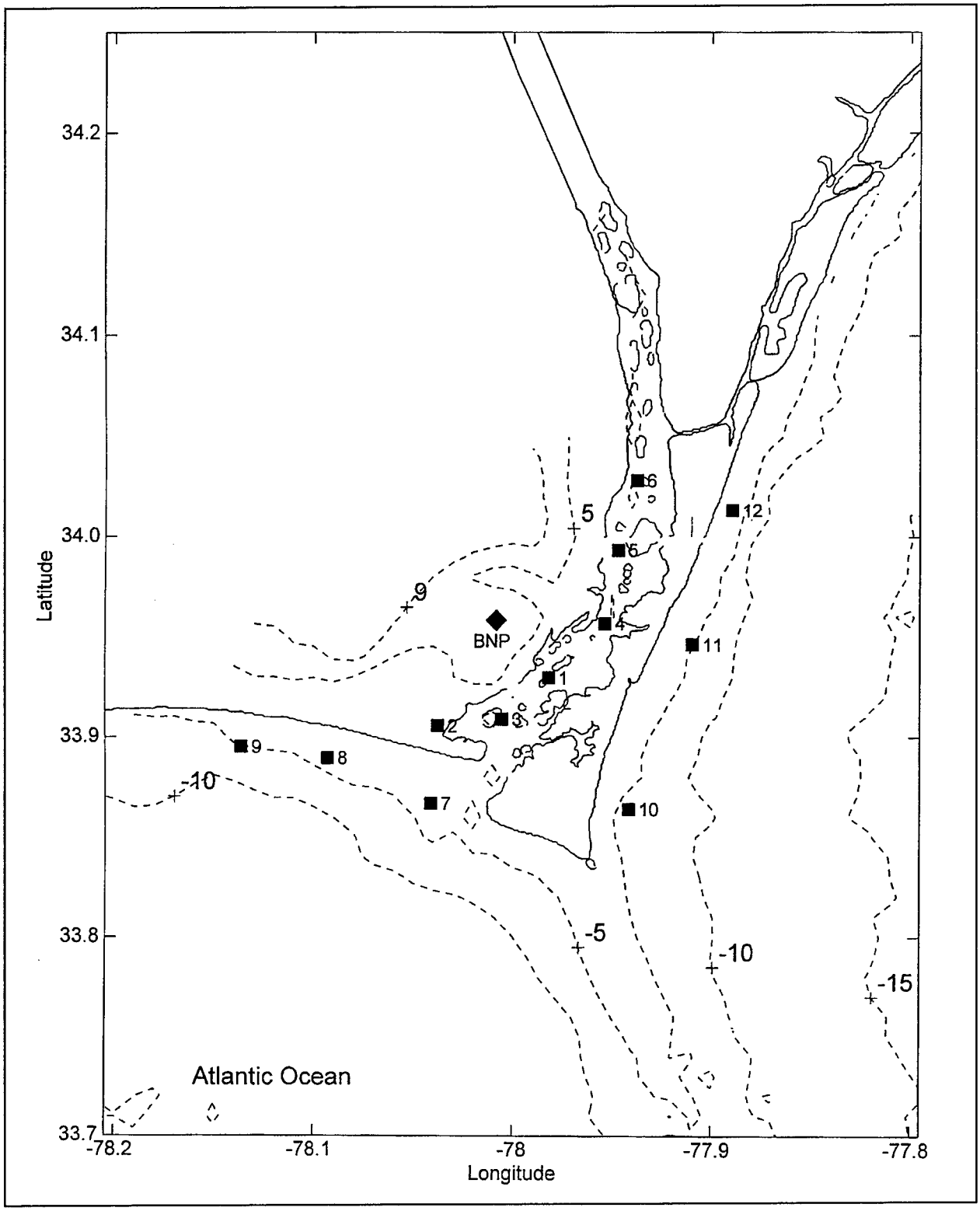

Figure 13. Location of 12 stations selected for storm-surge data analysis

Each simulation used a 30-sec time-step, and time-series of water-surface elevations were recorded at 15-min intervals at the 12 stations in the study area. Table 2 presents the computed peak storm-surge elevation at the selected 12 stations for the 24 historical and 2 hypothetical storms. The largest computed surge at the BNP site, which was 3.3 m, was caused by Hurricane Hazel, which directly impacted the study area in 1954.

Application of Wind-Wave Model

Adjacent weather systems were incorporated into PBL-generated wind fields supplied to the wave models in the same manner as those for the hindcast of Hurricane Hugo where wind velocities produced by the NCEP were used at all nodes lying beyond the periphery of the hurricane. However, this task was only performed for those seven storms occurring after 1980; winds were not available from the NCEP for prior storm periods.

Wave model simulations were performed for the same 24 historical tropical storms simulated with the storm-surge model. Wave conditions produced by Hurricane Hugo were used in place of the two hypothetical storms discussed in previous sections. Simulations were conducted in the same manner as with the Hurricane Hugo hindcast; simulations would be made using a coarse grid, and wave conditions would be saved and later used as boundary conditions in a subsequent simulation using the next finer grid.

Table 3 presents the averaged wave periods and wave heights along the Level 3 deepwater boundary under severe wave conditions for the 24 storms. Table 4 presents the maximum wave height computed at the 12 stations (specified in Table 2) in the vicinity of the BNP. Table 5 presents the wave-setup water-level elevation under severe wave condition at the 12 stations.

As shown in Table 5, wave effects are only significant on the ocean side of the shoreline where waves are breaking because of depth limitation. Inside the river, waves are generally very small because only a limited number of waves are able to propagate from the ocean into the river through the relatively narrow river entrance. As a result, the wave-induced setups are negligibly small along the river bank in the study area.

Application of EST Model

Input to the EST model consists of hurricane parameters and the associated peak total water-surface elevations produced with these parameters. Hurricane parameters are referred to as input vectors, whereas the peak total water surface elevations serve as the response vectors. The input data set containing these data is referred to as the training set of storms.

Table 3
Averaged Wave Periods and Wave Heights at the Level 3 Offshore Boundary

Case Number	Name	Wave Height, m	Wave Period, sec
1	Fran	8.8	12
2	Bertha	8.8	12
3	Hugo	6.8	12
4	Kate	3.6	9
5	Diana	3.7	9
6		3.0	9
7	Dennis	2.9	9
8	Agnes	7.2	9
9	Gladys	7.3	11
10	Dora	5.5	11
11	Donna	8.0	11
12	Gracie	3.4	11
13	Flossy	7.7	9
14	Hazel	8.8	11
15	Florence	7.1	11
16		3.0	9
17		7.5	11
18		7.8	11
19		6.8	11
20		5.7	11
21		6.8	11
22		6.7	11
23		7.7	11
24		7.6	11

Hurricane parameters used as input vectors are maximum wind speed, radius to maximum winds, atmospheric pressure anomaly or central-pressure deficit, translational or forward speed of the eye, track direction, and the minimum distance between the study area and the eye of the hurricane. Parameter values are selected at the time a hurricane makes its closet approach to the study area.

Table 4
Maximum Wave Height (m) at 12 Stations

Case	Station											
	1	2	3	4	5	6	7	8	9	10	11	12
1	0.03	0.02	0.12	0.00	0.00	0.00	1.88	2.26	2.01	1.63	1.63	1.76
2	0.02	0.02	0.09	0.00	0.00	0.00	1.22	1.42	1.46	1.18	1.19	1.32
3	0.03	0.15	0.15	0.02	0.00	0.00	1.42	1.64	1.45	1.30	1.37	1.37
4	0.02	0.02	0.09	0.00	0.00	0.00	1.10	1.37	1.20	0.64	0.65	0.69
5	0.02	0.04	0.06	0.03	0.00	0.00	0.72	0.94	0.84	0.89	1.03	0.98
6	0.00	0.00	0.03	0.00	0.00	0.00	0.75	0.89	0.80	0.42	0.43	0.47
7	0.01	0.01	0.05	0.00	0.00	0.00	0.81	0.90	0.88	0.54	0.54	0.60
8	0.02	0.02	0.10	0.00	0.00	0.00	1.50	1.73	1.60	0.70	0.76	0.81
9	0.01	0.00	0.07	0.00	0.00	0.00	1.86	2.05	1.95	0.99	0.96	1.01
10	0.02	0.02	0.09	0.00	0.00	0.00	1.38	1.72	1.49	1.02	0.99	1.11
11	0.01	0.00	0.07	0.00	0.00	0.00	1.83	2.03	1.97	1.24	1.20	1.31
12	0.00	0.01	0.05	0.00	0.00	0.00	0.81	0.97	0.89	0.66	0.63	0.73
13	0.03	0.02	0.14	0.00	0.00	0.00	2.19	2.42	2.16	0.49	0.90	0.97
14	0.11	0.71	0.36	0.04	0.00	0.02	2.20	2.58	2.36	1.86	2.06	2.06
15	0.02	0.02	0.12	0.00	0.00	0.00	1.98	2.29	1.99	0.52	0.90	0.85
16	0.00	0.00	0.04	0.00	0.00	0.00	0.79	0.92	0.89	0.69	0.67	0.75
17	0.03	0.02	0.13	0.00	0.00	0.00	2.27	2.44	2.32	0.98	1.02	1.07
18	0.02	0.02	0.11	0.00	0.00	0.00	1.87	2.21	2.00	1.48	1.43	1.63
19	0.02	0.01	0.10	0.00	0.00	0.00	1.91	2.03	1.97	0.63	0.80	0.79
20	0.00	0.00	0.05	0.00	0.00	0.00	1.33	1.58	1.44	0.85	0.83	0.91
21	0.01	0.01	0.08	0.00	0.00	0.00	1.84	2.04	1.92	0.56	0.76	0.74
22	0.04	0.11	0.18	0.01	0.00	0.00	1.78	2.06	1.86	1.19	1.24	1.24
23	0.01	0.01	0.08	0.00	0.00	0.00	1.83	2.00	1.99	1.44	1.37	1.54
24	0.03	0.02	0.13	0.00	0.00	0.00	2.24	2.22	2.11	1.07	1.11	1.1

Response vectors are the peak total water-surface elevations, which contain the effects of storm surge, wave setup, and tide. These effects are added linearly to depict the peak total water-surface elevation.

Table 5
Maximum Wave Setup Water-Level Elevation (m) at 12 Stations

Case	Station											
	1	2	3	4	5	6	7	8	9	10	11	12
1	0.00	0.00	0.00	0.00	0.00	0.00	0.01	0.17	0.23	0.12	0.03	0.05
2	0.00	0.00	0.00	0.00	0.00	0.00	0.00	0.15	0.06	0.21	0.08	0.35
3	0.00	0.00	0.00	0.00	0.00	0.00	0.00	0.00	0.00	0.00	0.00	0.06
4	0.00	0.00	0.00	0.00	0.00	0.00	0.00	0.03	0.02	0.01	0.01	0.05
5	0.00	0.00	0.00	0.00	0.00	0.00	0.00	0.01	0.01	0.00	0.00	0.01
6	0.00	0.00	0.00	0.00	0.00	0.00	0.00	0.01	0.00	0.00	0.00	0.01
7	0.00	0.00	0.00	0.00	0.00	0.00	0.00	0.00	0.01	0.00	0.00	0.00
8	0.00	0.00	0.00	0.00	0.00	0.00	0.00	0.11	0.10	0.00	0.10	0.33
9	0.00	0.00	0.00	0.00	0.00	0.00	0.00	0.17	0.13	0.03	0.02	0.12
10	0.00	0.00	0.00	0.00	0.00	0.00	0.00	0.05	0.05	0.14	0.04	0.17
11	0.00	0.00	0.00	0.00	0.00	0.00	0.00	0.17	0.13	0.48	0.28	0.41
12	0.00	0.00	0.00	0.00	0.00	0.00	0.00	0.00	0.00	0.00	0.00	0.00
13	0.00	0.00	0.00	0.00	0.00	0.00	0.00	0.07	0.06	0.00	0.02	0.09
14	0.00	0.00	0.00	0.00	0.00	0.00	0.00	0.00	0.01	0.58	0.15	0.22
15	0.00	0.00	0.00	0.00	0.00	0.00	0.00	0.08	0.07	0.00	0.00	0.00
16	0.00	0.00	0.00	0.00	0.00	0.00	0.00	0.01	0.01	0.00	0.00	0.01
17	0.00	0.00	0.00	0.00	0.00	0.00	0.00	0.09	0.08	0.06	0.03	0.13
18	0.00	0.00	0.00	0.00	0.00	0.00	0.00	0.04	0.05	0.06	0.03	0.15
19	0.00	0.00	0.00	0.00	0.00	0.00	0.00	0.09	0.08	0.08	0.05	0.18
20	0.00	0.00	0.00	0.00	0.00	0.00	0.00	0.15	0.12	0.09	0.04	0.20
21	0.00	0.00	0.00	0.00	0.00	0.00	0.00	0.15	0.12	0.01	0.03	0.12
22	0.00	0.01	0.00	0.00	0.00	0.00	0.00	0.01	0.00	0.00	0.00	0.15
23	0.00	0.00	0.00	0.00	0.00	0.00	0.00	0.11	0.09	0.11	0.05	0.27
24	0.00	0.00	0.00	0.00	0.00	0.00	0.00	0.15	0.13	0.01	0.00	0.02

The NHC database was processed to determine the necessary parameter values. Data contained in this database, however, are provided at 6-hr intervals. Therefore, for each storm in the training set, a cubic spline interpolation or curve-fitting procedure was followed to compute hurricane positions at hourly intervals. Using the interpolated hurricane positions, the minimum distance between the hurricane's track and the study area was determined. The required hurricane parameters were then interpolated from NHC's 6-hr incremental data.

In developing response vectors, peak storm-surge elevations were extracted from the storm-surge time-histories created by simulating the storms in the training set. Each surge elevation was then combined with four tidal elevations. The basis for this procedure is that a storm-surge event, and therefore its contribution to the peak total water-surface elevation, is independent of the tidal cycle. In other words, peak storm-surge levels can occur at any time during the tidal cycle. Thus, surge levels must be combined with a range of tidal elevations in order to accurately represent the temporal phasing of surge and tide.

Four tidal elevations were specified in the EST program for representing the tidal water-level component of the total water-surface elevations. One elevation represented high-tide elevations, whereas a second depicted low-tide levels. The two additional elevations equaled zero; thus, the combination of four elevations represents one tidal cycle. Furthermore, the EST program randomly chooses the tide elevation, based on the four elevations, in the simulation procedure. For this study, it was assumed that the maximum and minimum tidal elevations were equal to the M_2 constituent amplitude, which represents approximately 90 percent of the maximum tidal amplitude at the study area. The M_2 constituent amplitude was selected because it is more representative of the average tidal range occurring over a 1-month lunar cycle, specifying spring tide levels as the maximum tidal elevation (or neap tide levels as the minimum elevation) could cause biasing or unduly weighting the tidal water-level component towards extreme tidal elevations.

With four tidal elevations being specified with each set of input/response vectors, the total number of storms in the training set was effectively increased from 26 to 104 events. Using the EST model together with the augmented training set, 100 simulations, each modeling a 2,000-year period, were performed for each of the 12 stations in the study area. The frequency of occurrence for a hurricane to impact the study area is 0.216, or 24 storms over a 111-year period.

An example set of simulations is shown in Figure 14 for Station 1, located nearest to the BNP as indicated in Figure 8. Note that the figure displays curves for all 100 simulations in addition to the curve composed of 0's representing the mean value. Figure 15 presents the mean and error bands associated with Figure 14. Figure 15 is presented in a semilogarithm form to facilitate extrapolation to higher return periods. Although this practice is not recommended, it is recognized that the sponsor is required to make such estimates; therefore, final curves are presented in a form to facilitate such approximations.

One requirement of the NRC was to provide maximum surge-elevation estimates with return periods of 10,000, 100,000, and 1,000,000 years. It should be noted that predicted maximum surge elevations, regardless of the statistical analysis used in generating them (including the EST and JPM), are not reliable when their return periods exceed two to three times the time span over which the prototype data were collected. For this study, only 111 years of prototype data exist; therefore, surge levels having return periods exceeding 300 years should not be considered reliable.

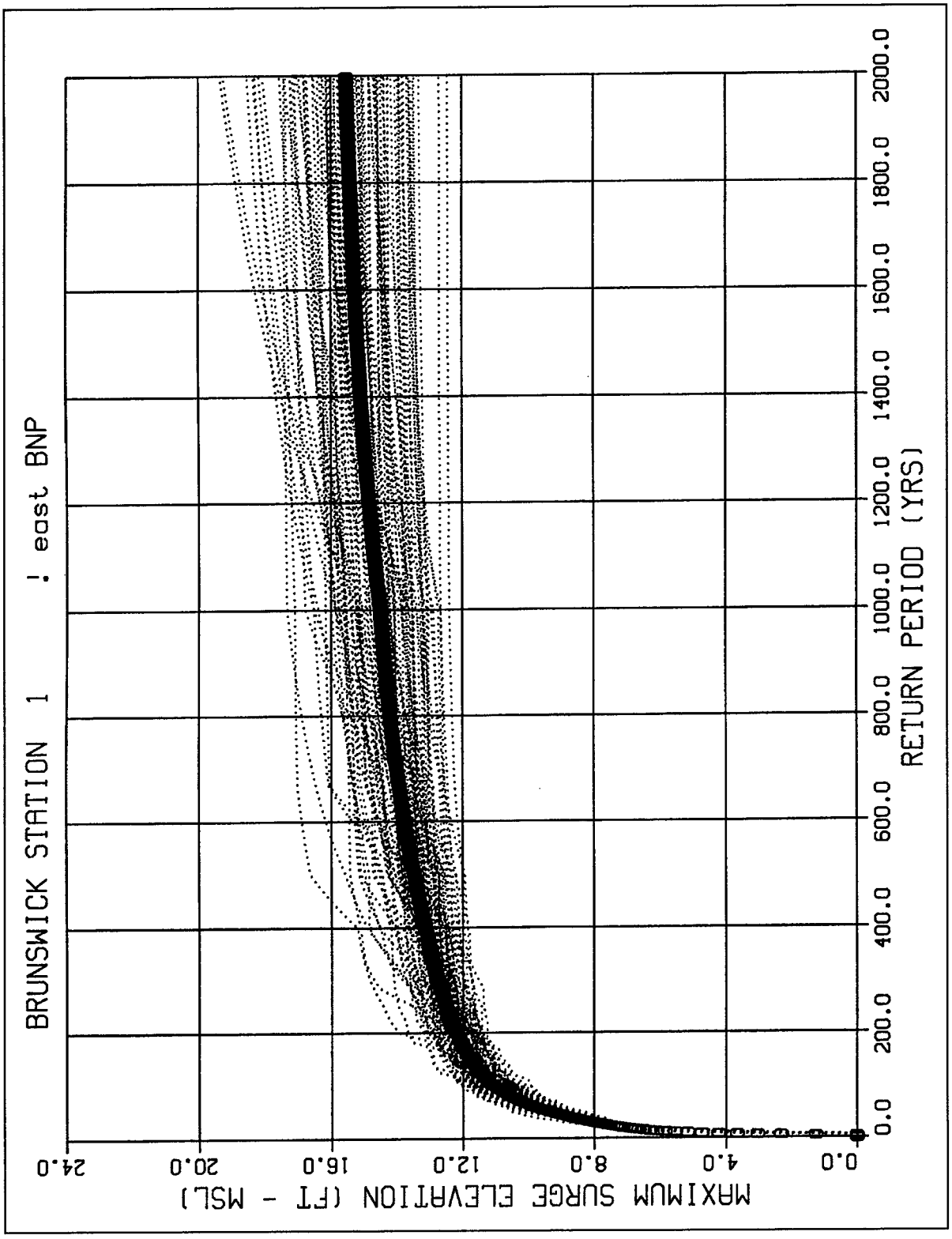

Figure 14. Frequency relationship for Station 1, near the BNP

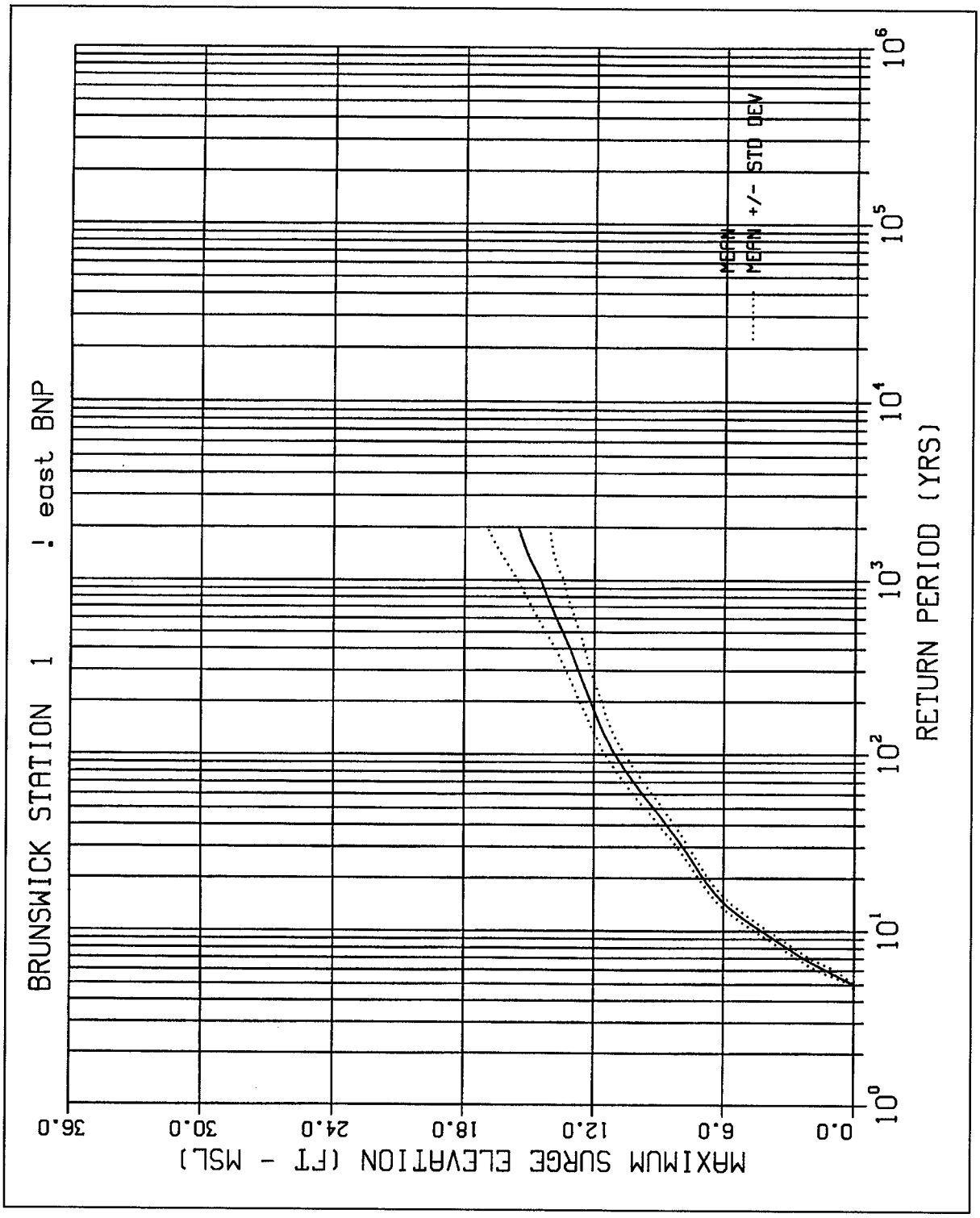

Figure 15. Mean value/standard deviation relationships for Station 1

Total maximum surge elevations for all 12 locations are presented in Appendix A, and all semilogarithm plots are presented in Appendix B. Table 6 presents estimated total surge values for frequency relationships for return periods of 10,000, 100,000, and 1,000,000 years. These estimates were computed, via linear extrapolation, using the 200- and 1,000-year return period total maximum surge elevations. Because the extrapolation is linear, they can be considered very conservative, and as previously mentioned, the available prototype data do not support estimates on this order of magnitude.

Table 6
Extrapolated Frequency Relationships for Stations 1-12

Stations	Return Period 10,000 years	Return Period 100,000 years	Return Period 1,000,000 years
1	18.0	21.4	24.6
2	19.1	23.0	27.2
3	18.4	22.4	26.3
4	19.1	23.3	27.6
5	20.7	25.5	30.4
6	20.4	25.2	30.0
7	18.0	22.3	26.7
8	18.9	23.3	27.8
9	19.2	23.9	28.5
10	16.8	20.6	24.3
11	14.8	18.2	21.3
12	15.7	19.1	22.4

7 Comparison of Analyses

Designed during the late 1960s, the BNP was constructed with a design basis flood level of 22.0 ft MSL. This level was determined by predicting, using Bathystropic Storm Surge Theory (BSST), surge elevations induced by the PMH. The PMH is a hypothetical hurricane that is constructed such that it is the most severe storm that is reasonably possible for a particular region and that it approaches a site along a particular path and at an optimal speed so that it produces the greatest surge level when compared with all other possible storms.

The BSST provides a one-dimensional storm-surge solution where surge levels are computed along a transect that begins at the continental shelf break and ends at the coast. The governing equations, compared with those in ADCIRC, are simplified mathematically by excluding terms that are either small, relative to other terms in the equations, or are negligible. For example, convection and diffusion are neglected. Whereas the one-dimensional assumption can be valid for open-coast regions where shoreline alignment is relatively straight and bathymetric/topographic gradients run parallel to the shore, the BSST cannot be used in areas of abrupt changes in shoreline configuration or in the bathymetric gradients. For example, the BSST should not be applied to estuaries or inshore of barrier islands.

Although BSST methods can be considered obsolete because present computer technology permits more rigorous mathematical analyses using two- and three-dimensional computer models, the BSST method was an accepted procedure in the engineering field for estimating storm surge at the time the BNP was planned. Furthermore, the methodology used in the plant design met the regulations governing hurricane storm-surge calculations for nuclear power plant design, outlined in Regulatory Guide 1.59, Design Basis Floods for Nuclear Power Plants (RG 1.59, Regulatory Guide 1977).

This RG states that approved detailed PMH analyses are an acceptable approach to developing design criteria. Additionally, RG 1.59 provides probable maximum storm-surge estimates for both the Atlantic and Gulf coasts. These estimates are the recognized licensing design basis for the BNP.

In 1992, NOAA published a study entitled "A Storm Surge Atlas for the Myrtle Beach, South Carolina, and Wilmington, North Carolina, Area" that delineates limits of inundation caused by hurricane-induced flooding in the subject area. This study found that a severe hurricane could induce a surge elevation of 28.4 ft MSL at the BNP site, or 6.4 ft above the plant's design basis flood level.

NOAA employed the Sea, Lake and Overland Surges from Hurricanes (SLOSH) model in making their assessment. Developed in the 1960s and 1970s, SLOSH is a two-dimensional, finite-difference model for solving the conservation of mass and Navier-Stokes equations, which depict fluid motion. Study regions are defined in the model using a polar coordinate grid. Cell dimensions at the BNP measure approximately 0.85 by 0.85 mile.

Inundation limits and accompanying surge elevations presented in the NOAA report were obtained by simulating 1,450 hypothetical hurricanes. Furthermore, the JPM was used in synthesizing these storms to describe storm attributes or parameters. These parameters are forward speed, intensity, propagation direction (storms along parallel tracks), track, and landfall position. Employing a statistical analysis of historical storms, and assuming independence of storm parameters, a PDF is created for each parameter. A range of values is chosen from the density function for each attribute, together with their respective probability of occurrence, and a series of hypothetical hurricanes are then synthesized by combining various parameter values. The probability of occurrence for a particular storm is the product of the probabilities associated with each individual parameter used in synthesizing that storm.

The surge value of 28.4 ft MSL at the BNP site is based on a combination of storm parameters consistent with an extreme hurricane, with a corresponding low frequency of occurrence. This storm, however, may not be realistic because hurricane parameters were assumed to be independent from one another and may be a product of an unrealistic combination of storm parameters or have a correspondingly negligible probability of occurrence.

Additionally, the grid used in the SLOSH simulations may not have incorporated certain roadways in the vicinity of the BNP site. These roadways may act as a levee in the study area, impeding or blocking the propagation of storm surge into the area. In a study contracted by the Carolina Power and Light Corporation (the operator of the BNP), Dr. R. A. Luettich, Jr., Associate Professor, University of North Carolina, Institute of Marine Science, reviewed the NOAA study and found that the particular synthetic hurricane that induced the 28.4 ft MSL surge followed a northeasterly path. He noted that, along this path, Highways 211, 87, and 133 could act as levees, impeding storm-surge propagation into the study area.

Furthermore, Dr. Luettich noted that surge inundation limits predicted by the model show significant surge in the region beyond these highways, suggesting that they may not be properly specified in the model. Dr. Luettich was unable to investigate whether these highways were correctly specified in the model because NOAA refused to release its model to him.

Because of the uncertainties in the above reports, the BNP made an independent assessment of the NOAA report and initiated a new set of calculations based on the PMH criteria. One task of the present study is to evaluate the results of the BNP calculation to determine if the design basis flood level based on those calculations provides an adequate measure of safety for the BNP.

The original frequency study used the Standard Project Hurricane (SPH) model to define wind and pressure fields associated with the parameterized PMH. The SPH model is a quasi-empirical model that computes wind and pressure as a function of specified hurricane criteria, such as pressure deficit, radius to maximum winds, maximum wind, forward speed, and path. The PBL model used in current CHL applications is physics based and requires eye location and central pressure input only. All additional parameters are implied or computed from this information. Therefore, CHL does not support a hurricane model that is precisely compatible with the SPH technology. However, wind and atmospheric pressure fields consistent with the SPH were approximated using the PBL model and subsequently used as input to the ADCIRC model.

For approximating the SPH, Hurricane Hazel was selected because this event was similar in trajectory and speed to the hypothetical SPH. This hurricane, which occurred in October 1954, was the storm of record for the study area. The central pressure measured for Hurricane Hazel was altered to generate a PMH-like storm event for the PBL model. Also, the position of the landfall point was altered in order to impose a critical path for producing the greatest surge at the study site. Using these wind and pressure fields, Hurricane Hazel was then simulated using the ADCIRC model to compute surge elevations.

Surge levels discussed above were compared with the design basis flood levels used in constructing the BNP and are the basis for determining whether the PMH-based maximum storm-surge elevation provides an adequate safety margin against storm-surge flooding. Table 7 presents comparison of the BNP and RG 1.59 design storms and the result from ADCIRC. The RG 1.59 estimates shown in Table 7 are based on data for Raleigh Bay, North Carolina (north of the BNP site).

This comparison shows that the estimated maximum total storm surge computed in the present study is essentially the same as that obtained in the original BNP and RG 1.59 studies. This indicates that the design basis flood level computed in designing the BNP is appropriate for the input storm parameters specified. As will be concluded in the following chapter, the BNP design basis flood level therefore provides an adequate margin of safety against inundation by tropical storm surge.

Table 7
Comparison of Design Storms

Parameter	BNP	RG 1.59	ADCIRC
CPI, in Hg	26.86	26.89	26.88
Radius of max. winds, mile	30	35	25
Max. sustained winds, mph	128	130-149	-
Forward speed, mph	10-30	5-38	21-43
Astronomical tide, m, MSL	1.43	1.77	1.77
Path (deg) cw from north	160	135	180
Max. surge, m	6.71	6.69	6.43
Wave effect, m	1.25	1.25[a]	1.25[a]
Total surge, m	7.96	7.94	7.68

[a] According to BNP design criteria. Wave effect includes wave-breaking height, setup, and runup.

8 Summary and Conclusions

A hurricane stage-frequency analysis was conducted for the Brunswick, North Carolina, Nuclear Plant. The purpose of this study was to determine realistic frequency-of-occurrence relationships for this site using the EST and to evaluate the results of two previous analyses. The first study used the PMH for estimating peak total water-surface elevations at the BNP, and results of this study were used in defining the plant's design basis flood level. The second study used the JPM in its statistical analysis and produced a peak total water-surface level that was 6.4 ft above the plant's design basis flood level. The purpose of this comparison was to determine if the design basis flood level determined in the original surge study provides the BNP an adequate margin of safety against inundation induced by tropical storm surges.

Four models were employed in this analysis, including a wind and atmospheric pressure field model, a long-wave hydrodynamic model, a wind-generation wave model, and an empirical simulation model. The PBL model was used for generating hurricane-induced wind and atmospheric pressure fields subsequently used as input to the wave and hydrodynamic models. Data supplied to the PBL model were obtained from the NHC's HURDAT database.

The ADCIRC numerical model was used for simulating the long-wave hydrodynamic processes in the study area. This program employs a two-dimensional, depth-integrated, finite-element solution of the GWCE. The fundamental components of the GWCE equation are the depth-integrated continuity and Navier-Stokes equations for conservation of mass and momentum. Furthermore, model validation was achieved by performing a storm-surge simulation of Hurricane Hugo, which impacted the study area in 1989.

WISWAVE is a discrete directional spectral wave model where the spectral wave-height computations are based on integration of energy over the discrete frequency spectrum. Model output include time-series of significant wave height, peak (dominant) or mean wave period, and mean wave direction. This model also was validated using Hurricane Hugo.

The EST procedure was used for determining the stage-frequency relationships. The EST is a statistical resampling procedure that uses historical data to develop joint probability relationships among the various measured storm parameters (e.g., maximum wind speed). The EST generates a database of peak storm-surge elevations by simulating multiple-year periods (e.g. 2,000-year

periods) of storm activity a multiple number of times. Stage-frequency relationships are then generated using the model-generated peak storm-surge elevations and wave setups together with tidal elevations.

The EST was developed to overcome difficulties associated with frequency analyses based on hypothetical events constructed from the random combination of storm parameters and the subsequent assumption of parameter independence, such as the JPM. The EST-based approach has a demonstrated capability of generating reliable storm-induced stage-frequency estimates and has been applied in numerous frequency studies within the USACE. As a result of these successful applications, the EST has been chosen as the preferred frequency analysis methodology for developing design criteria by the USACE.

The EST methodology is described in Borgman and Scheffner (1991) and Scheffner and Borgman (1992) and has been used in 14 USAE-sponsored studies, including the following: Coast of Delaware Hurricane Stage-Frequency Analysis (Mark and Scheffner 1997); New York Bight Mud Dump - Vertical Erosion Frequency Analysis (Scheffner and Clausner 1996); Fire Island to Montauk Point, Long Island, New York, Tropical and Extratropical Storm Stage-Frequency Analysis (Scheffner and Mark 1997); Lake Pontchartrain Hurricane Stage-Frequency Analysis (Scheffner, Mark, and Brown 1998a); Morganza, Louisiana, to the Gulf of Mexico Hurricane Stage-Frequency Analysis (Scheffner, Mark, and Brown 1998b); South River, New York, Stage-Frequency Analysis (Letter, in preparation); Dredged Material Management Plan (DMMP) for the Port of New York and New Jersey - Modeling Studies to Support Island CDF and Constructed CAD Pit Design (Ebersole et al. 1998); Hurricane Induced Stage-Frequency Relationships for the Territory of American Samoa (Militello and Scheffner 1998); Kivalina, Alaska, Extratropical Storm Surge Analysis (Scheffner and Miller, in preparation); Lake Okeechobee Hurricane Stage-Frequency Analysis (U.S. Army Engineer (USAE) District, Jacksonville 1995); Brevard County, Florida, Dune/ Shoreline Recession Analysis (USAE District, Jacksonville 1996); Fort Pierce, Florida, Dune/Shoreline Recession Analysis (USAE District, Jacksonville 1998a); Saint Johns County, Florida, Dune/Shoreline Recession Analysis (USAE District, Jacksonville 1998b); and Ponce Inlet, Florida, Dune/Shoreline Recession Analysis (USAE District, Jacksonville 1998c).

Results of the present analysis show that the design basis flood level at which the BNP was constructed is adequate to ensure that safety margins protecting against extreme hurricane-induced storm-surge flooding are maintained. The EST analysis predicted that a 2,000-year return period event induces a total surge (combined storm surge, wave setup, and tide) elevation of 16 to 17 ft MSL. This elevation is 5 ft lower than the 22-ft design basis flood elevation, which was computed using the PMH. (The PMH is estimated to produce a total surge level that has a return period of 2,000 years and is the basis for defining the design basis flood elevation.)

This analysis also indicates that a total surge level of 22 ft MSL has a return period of approximately 100,000 years (which is the design elevation of the BNP). Because this analysis employed the EST, these estimates are based on prototype data and should be considered more realistic than results based on hypothetically

constructed events, such as the JPM. For example, the EST produced a 100-year total surge elevation of approximately 11 to 12 ft at three stations in the vicinity of the BNP; this surge elevation is consistent with historical data.

Overall conclusions of the present study are that previous studies are overly conservative with respect to the frequencies associated with a given surge elevation. This conclusion is consistent with the fact that the hypothetical storms used in the JPM-based frequency studies do not realistically replicate the historic storms experienced in the study region. Although storms synthesized using the JPM technique may be similar to historic storms (in track, intensity, etc.), the probability of occurrence assigned to JPM-generated storms can be greater than the probability of occurrence of the historic storms; essentially, the JPM method predicts more intense storms occurring more frequently than what the historic data support. The present analysis shows that this appears to be the case for the BNP site.

References

Borgman, L., Miller, M., Butler, L., and Reinhard, R. (1992). "Emperical simulation of future hurricane storm histories as a tool in engineering and economic analysis." *Fifth International Conference on Civil Engineering in the Oceans.* ASCE, College Station, TX, 2-5 November 1992.

Borgman, L. E., and Scheffner, N. W. (1991). "Simulation of time sequences of wave height, period, and direction," Technical Report DRP-91-2, U.S. Army Engineer Waterways Experiment Station, Vicksburg, MS.

Cardone, V. J., Greenwood, C. V., and Greenwood, J. A. (1992). "Unified program for the specification of hurricane boundary layer winds over surfaces of specified roughness," Contract Report CERC-92-1, U.S. Army Engineer Waterways Experiment Station, Vicksburg, MS.

Ebersole, B. A., et al. (1998). "Dredged Material Management Plan (DMMP) for the Port of New York and New Jersey - Modeling studies to support island CDF and constructed CAD pit design," Technical Report (draft), U.S. Army Engineer Waterways Experiment Station, Vicksburg, MS.

Flather, R. A. (1988). "A numerical model investigation of tides and diurnal-period continental shelf waves along Vancouver Island," *Journal of Physical Oceanography* 18, 115-139.

Garrat, J. R. (1977). "Review of drag coefficients over oceans and continents," *Monthly Weather Review 105*, 915-929.

Gumbel, E. J. (1954). *Statistical theory of extreme values and some practical applications; a series of lectures.* U.S. Government Printing Office, Washington, DC.

Jarvinen, B. R., Neumann, C. J., and Davis, M. A. (1988). "A tropical cyclone data tape for the North Atlantic Basin, 1886-1983: Contents, limitations, and uses," NOAA Technical Memorandum NWS NHC 22, National Hurricane Center, Miami, FL.

Jelesnianski, C. P., and Taylor, A. D. (1973). "A preliminary view of storm surges before and after storm modifications," NOAA Technical Memorandum ERL WMPO-3, Weather Modification Program Office, Boulder, CO.

Kolar, R. L., Gray, W. G., Westerink, J. J., and Luettich, R. A. (1993). "Shallow water modeling in spherical coordinates: Equation formulation, numerical implementation, and application," *Journal of Hydraulic Research.*

Letter, J. "South River, New York, stage-frequency analysis," Miscellaneous Paper in preparation, U.S. Army Engineer Waterways Experiment Station, Vicksburg, MS.

Luettich, R. A., Jr., Westerink, J. J., and Scheffner, N. W. (1992). "ADCIRC: An advanced three-dimensional circulation model for shelves, coasts, and estuaries," Technical Report DRP-92-6, U.S. Army Engineer Waterways Experiment Station, Vicksburg, MS.

Mark, D. J., and Scheffner, N. W. (1997). "Coast of Delaware hurricane stage-frequency analysis," Miscellaneous Paper CHL-97-1, U.S. Army Engineer Waterways Experiment Station, Vicksburg, MS.

Millitello, A., and Scheffner, N. W. (1998). "Hurricane-induced stage-frequency relationships for the territory of American Samoa," Technical Report CHL-98-33, U.S. Army Engineer Waterways Experiment Station, Vicksburg, MS.

Scheffner, N. W., and Borgman, L. E. (1996). "A stochastic time series representation of wave data," *J. Wtrwy. Port, Coast. and Oc. Engrg.* 118(4), 337-351.

Scheffner, N. W., and Borgman, L. E. (1996). "Application of large domain hydrodynamic models to generate frequency-of-occurrence relationships," Estuarine and Coastal Modeling.

Scheffner, N. W. and Clausner, J. (1996). "New York Bight Mud Dump - Vertical Erosion Frequency Analysis," Miscellaneous Paper (draft), U.S. Army Engineer Waterways Experiment Station, Vicksburg, MS.

Scheffner, N. W., and Mark, D. J. (1997). "Fire Island to Montauk Point, Long Island, New York, tropical and extratropical storm stage-frequency analysis," Miscellaneous Paper (draft), U.S. Army Engineer Waterways Experiment Station, Vicksburg, MS.

Scheffner, N. W., Mark, D. J., Blain, C. A., Westerink, J. J., and Luettich, R. A., Jr. (1994). "ADCIRC: An advanced three-dimensional circulation model for shelves, coasts, and estuaries; Report 5, A tropical storm database for the east and Gulf of Mexico coasts of the United States," Technical Report DRP-92-6, U.S. Army Engineer Waterways Experiment Station, Vicksburg, MS.

Scheffner, N. W., Mark, D. J., and Brown, M. (1998). "Lake Pontchartrain hurricane stage-frequency analysis," Miscellaneous Paper (draft), U.S. Army Engineer Waterways Experiment Station, Vicksburg, MS.

_____. (1998). "Morganza, Louisiana, to the Gulf of Mexico hurricane stage-frequency analysis," Miscellaneous Paper (draft), U.S. Army Engineer Waterways Experiment Station, Vicksburg, MS.

Scheffner, N. W., and Miller, M. C. (1998). "Kivalina, Alaska, extratropical storm surge analysis," Miscellaneous Paper in preparation, U.S. Army Engineer Waterways Experiment Station, Vicksburg, MS.

U.S. Army Engineer District, Jacksonville (1995). "Lake Okeechobee hurricane stage-frequency analysis," U.S. Army Engineer Division, South Atlantic, Jacksonville, FL.

_____. (1996). "Brevard County, Florida, dune/shoreline recession analysis," U.S. Army Engineer Division, South Atlantic, Jacksonville, FL.

_____. (1998a). "Fort Pierce, Florida, dune/shoreline recession analysis," (in preparation), U.S. Army Engineer Division, South Atlantic, Jacksonville, FL.

_____. (1998b). "Saint Johns County, Florida, dune/shoreline recession analysis," (in preparation), U.S. Army Engineer Division, South Atlantic, Jacksonville, FL.

_____. (1998c). "Ponce Inlet, Florida, dune/shoreline recession analysis," (in preparation), U.S. Army Engineer Division, South Atlantic, Jacksonville, FL.

Westerink, J. J., Luettich, R. A., Baptista, A. M., Scheffner, N. W., and Farrar, P. (1992). "Tide and storm surge predictions using finite element model," *Journal of Hydraulic Engineering*, American Society of Civil Engineers, 118(10), 1373-1390.

Appendix A
Stage-Frequency Relationship Tables

Table A1
Stage-Frequency Relationship for Station 1

Return Period, years	Water-Surface Elevation, ft MSL	Standard Deviation, ft
10	4.23	0.35
25	7.46	0.25
50	9.23	0.41
100	11.02	0.47
200	12.19	0.52
500	13.48	0.83
750	14.11	0.94
1,000	14.50	1.07
1,500	15.19	1.25
2,000	15.54	1.45

Table A2
Stage-Frequency Relationship for Station 2

Return Period, years	Water-Surface Elevation, ft MSL	Standard Deviation, ft
10	3.44	0.35
25	6.93	0.32
50	9.01	0.41
100	10.74	0.52
200	12.21	0.70
500	13.86	1.04
750	14.60	1.18
1,000	15.06	1.29
1,500	16.07	1.47
2,000	16.58	1.71

Table A3
Stage-Frequency Relationship for Station 3

Return Period, years	Water-Surface Elevation, ft MSL	Standard Deviation, ft
10	3.29	0.32
25	6.60	0.30
50	8.59	0.44
100	10.38	0.53
200	11.84	0.65
500	13.44	0.98
750	14.18	1.10
1,000	14.65	1.18
1,500	15.60	1.41
2,000	16.07	1.67

Table A4
Stage-Frequency Relationship for Station 4

Return Period, years	Water-Surface Elevation, ft MSL	Standard Deviation, ft
10	3.72	0.34
25	7.40	0.30
50	9.19	0.35
100	10.70	0.43
200	12.02	0.59
500	13.63	0.86
750	14.47	0.97
1,000	15.04	1.28
1,500	16.17	1.66
2,000	16.74	2.12

Table A5
Stage-Frequency Relationship for Station 5

Return Period, years	Water-Surface Elevation, ft MSL	Standard Deviation, ft
10	3.88	0.39
25	7.71	0.29
50	9.35	0.31
100	10.86	0.46
200	12.30	0.58
500	14.23	1.00
750	15.14	1.17
1,000	15.83	1.48
1,500	17.15	1.86
2,000	17.82	2.33

Table A6
Stage-Frequency Relationship for Station 6

Return Period, years	Water-Surface Elevation, ft MSL	Standard Deviation, ft
10	3.99	0.38
25	7.77	0.33
50	9.52	0.34
100	11.01	0.45
200	12.41	0.58
500	14.36	0.92
750	15.18	1.05
1,000	15.75	1.25
1,500	16.79	1.52
2,000	17.32	1.84

Table A7
Stage-Frequency Relationship for Station 7

Return Period, years	Water-Surface Elevation, ft MSL	Standard Deviation, ft
10	2.43	0.24
25	5.24	0.29
50	7.07	0.43
100	8.87	0.58
200	10.56	0.68
500	12.34	0.96
750	13.07	1.03
1,000	13.61	1.22
1,500	14.51	1.45
2,000	14.96	1.70

Table A8
Stage-Frequency Relationship for Station 8

Return Period, years	Water-Surface Elevation, ft MSL	Standard Deviation, ft
10	2.81	0.22
25	5.65	0.29
50	7.56	0.44
100	9.47	0.58
200	11.21	0.69
500	13.06	1.06
750	13.88	1.14
1,000	14.47	1.36
1,500	15.45	1.56
2,000	15.94	1.82

Table A9
Stage-Frequency Relationship for Station 9

Return Period, years	Water-Surface Elevation, ft MSL	Standard Deviation, ft
10	2.72	0.23
25	5.64	0.29
50	7.61	0.45
100	9.57	0.61
200	11.38	0.70
500	13.24	1.00
750	14.06	1.11
1,000	14.63	1.32
1,500	15.58	1.52
2,000	16.06	1.77

Table A10
Stage-Frequency Relationship for Station 10

Return Period, years	Water-Surface Elevation, ft MSL	Standard Deviation, ft
10	2.35	0.28
25	5.41	0.34
50	7.40	0.42
100	9.04	0.44
200	10.34	0.52
500	11.85	0.92
750	12.52	0.98
1,000	13.01	1.16
1,500	13.89	1.42
2,000	14.34	1.68

Table A11
Stage-Frequency Relationship for Station 11

Return Period, years	Water-Surface Elevation, ft MSL	Standard Deviation, ft
10	2.38	0.25
25	5.29	0.31
50	7.01	0.34
100	8.35	0.38
200	9.51	0.53
500	10.84	0.76
750	11.40	0.83
1,000	11.73	0.89
1,500	12.40	1.07
2,000	12.74	1.27

Table A12
Stage-Frequency Relationship for Station 12

Return Period, years	Water-Surface Elevation, ft MSL	Standard Deviation, ft
10	2.86	0.26
25	5.80	0.32
50	7.48	0.32
100	8.81	0.38
200	9.96	0.55
500	11.36	0.84
750	11.94	0.88
1,000	12.29	0.98
1,500	13.12	1.14
2,000	13.53	1.39

Appendix B
Graphs of Stage-Frequency Relationships

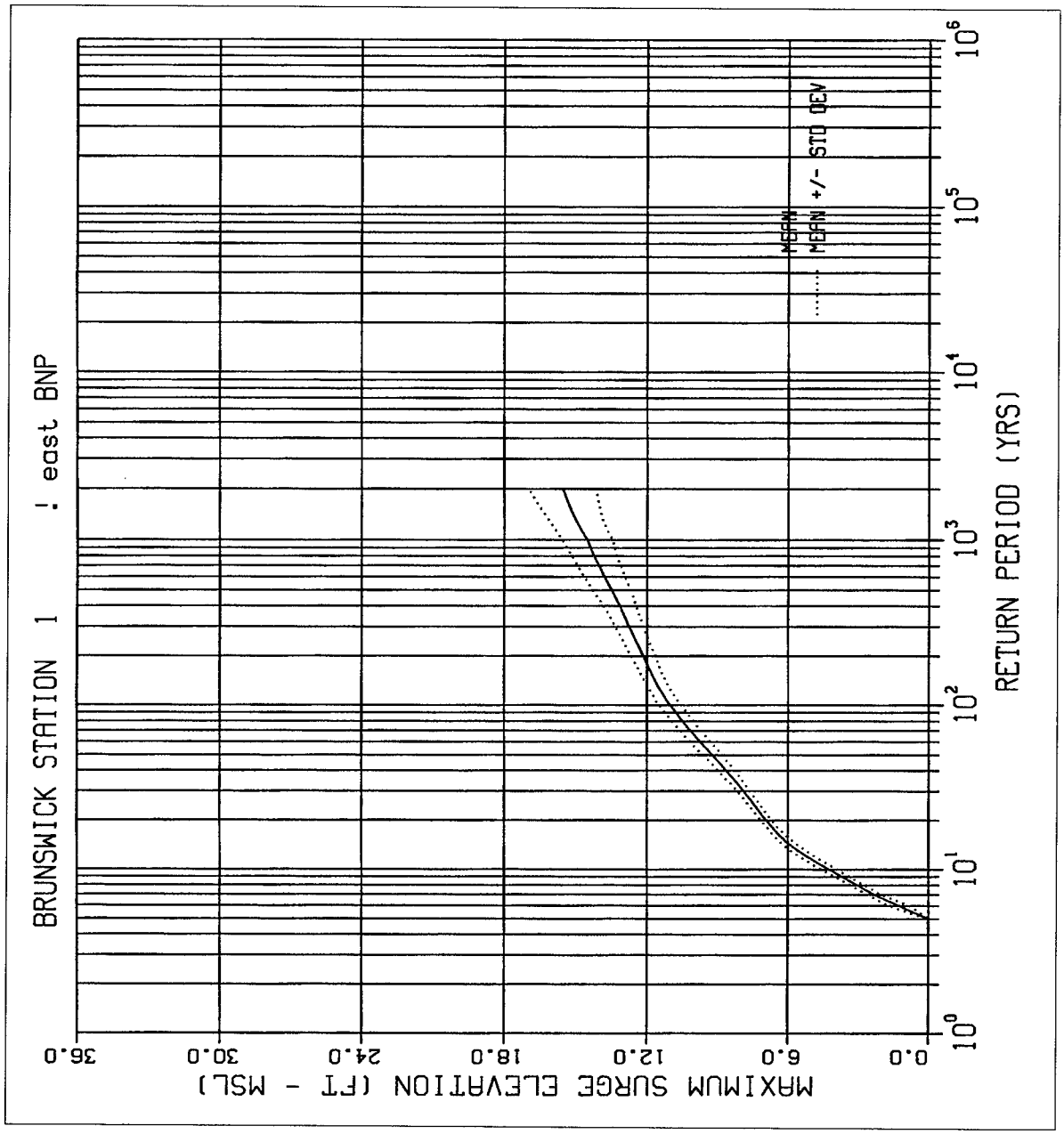

Figure B1. Stage-frequency relationship for Station 1

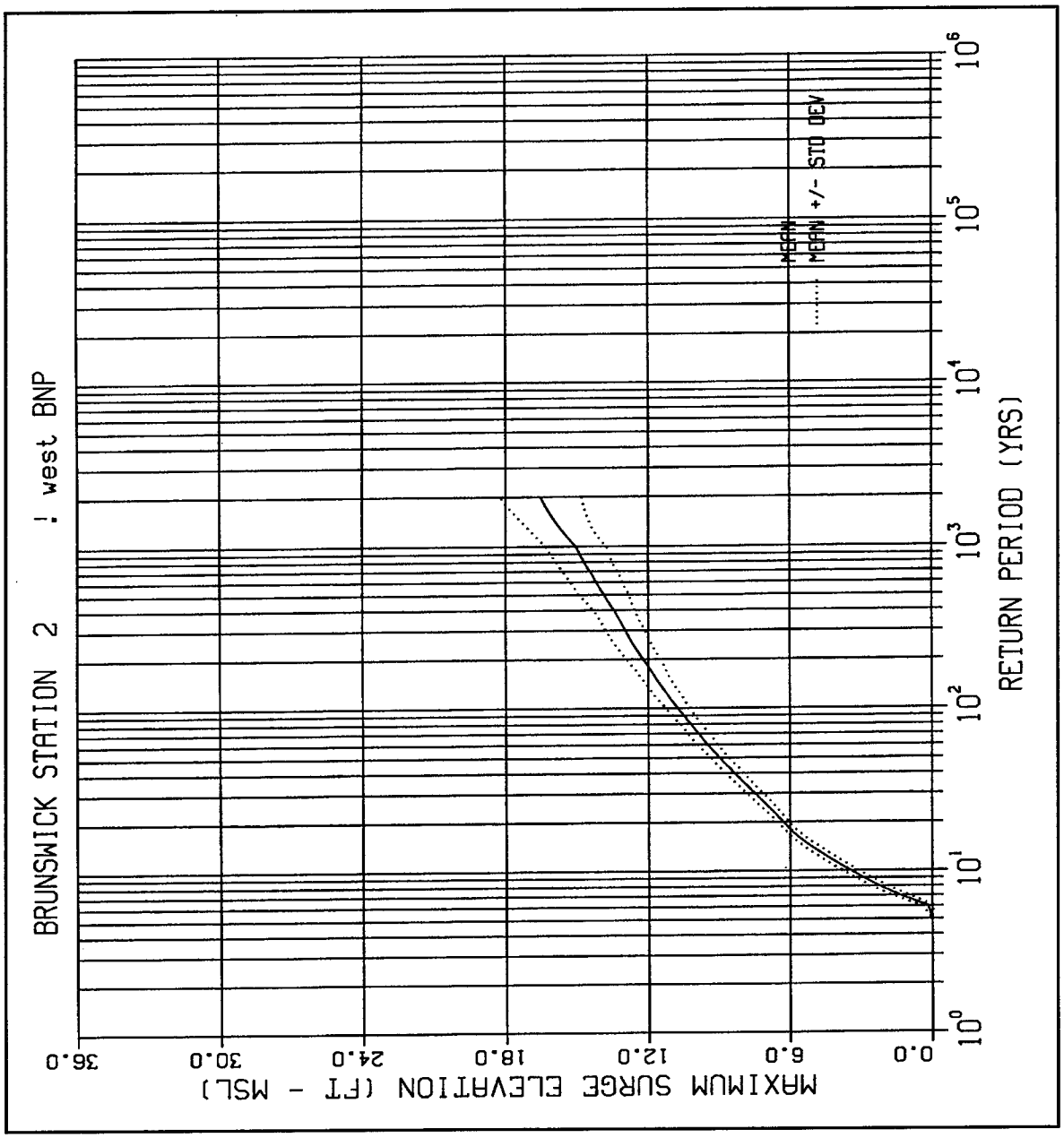

Figure B2. Stage-frequency relationship for Station 2

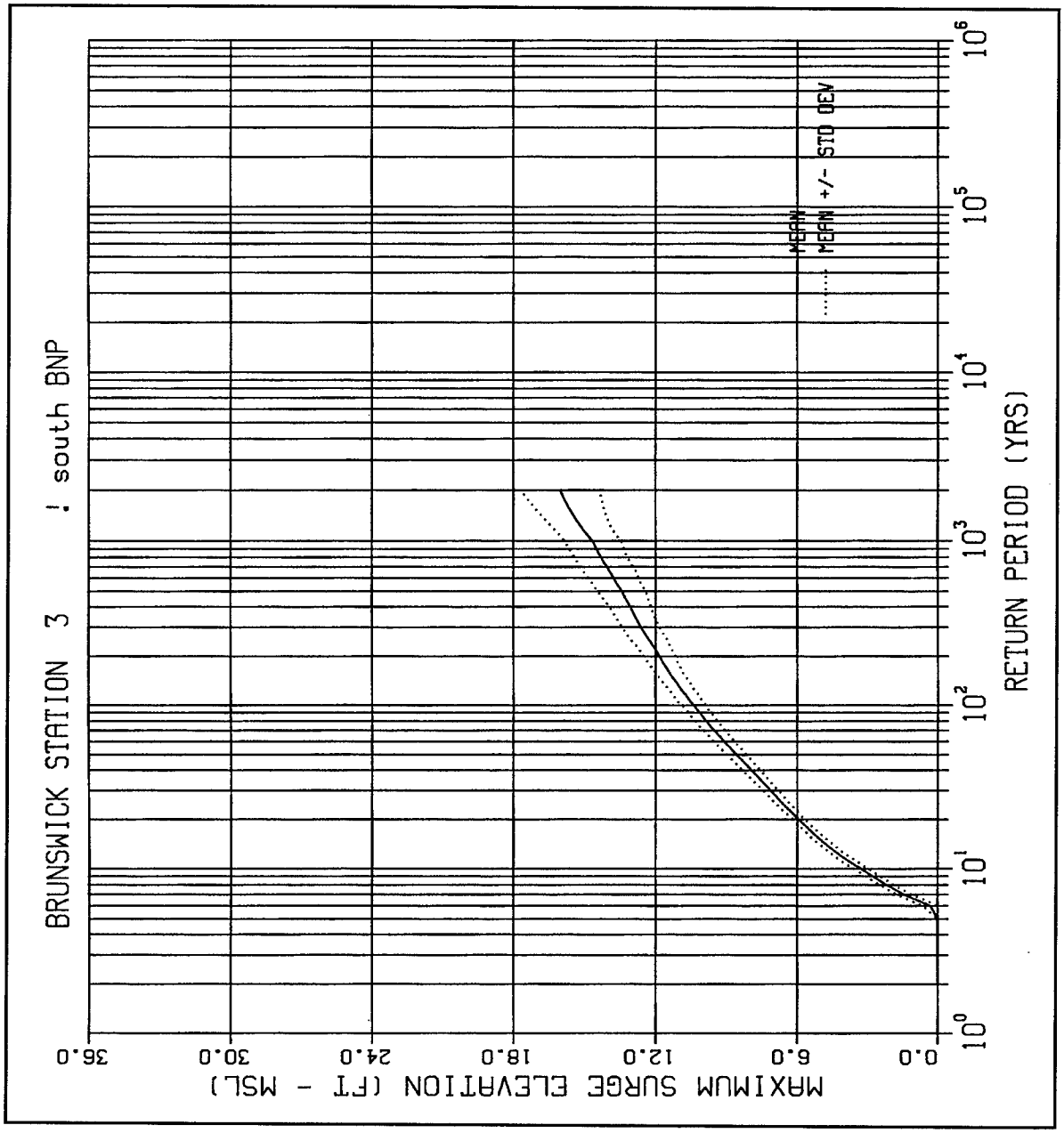

Figure B3. Stage-frequency relationship for Station 3

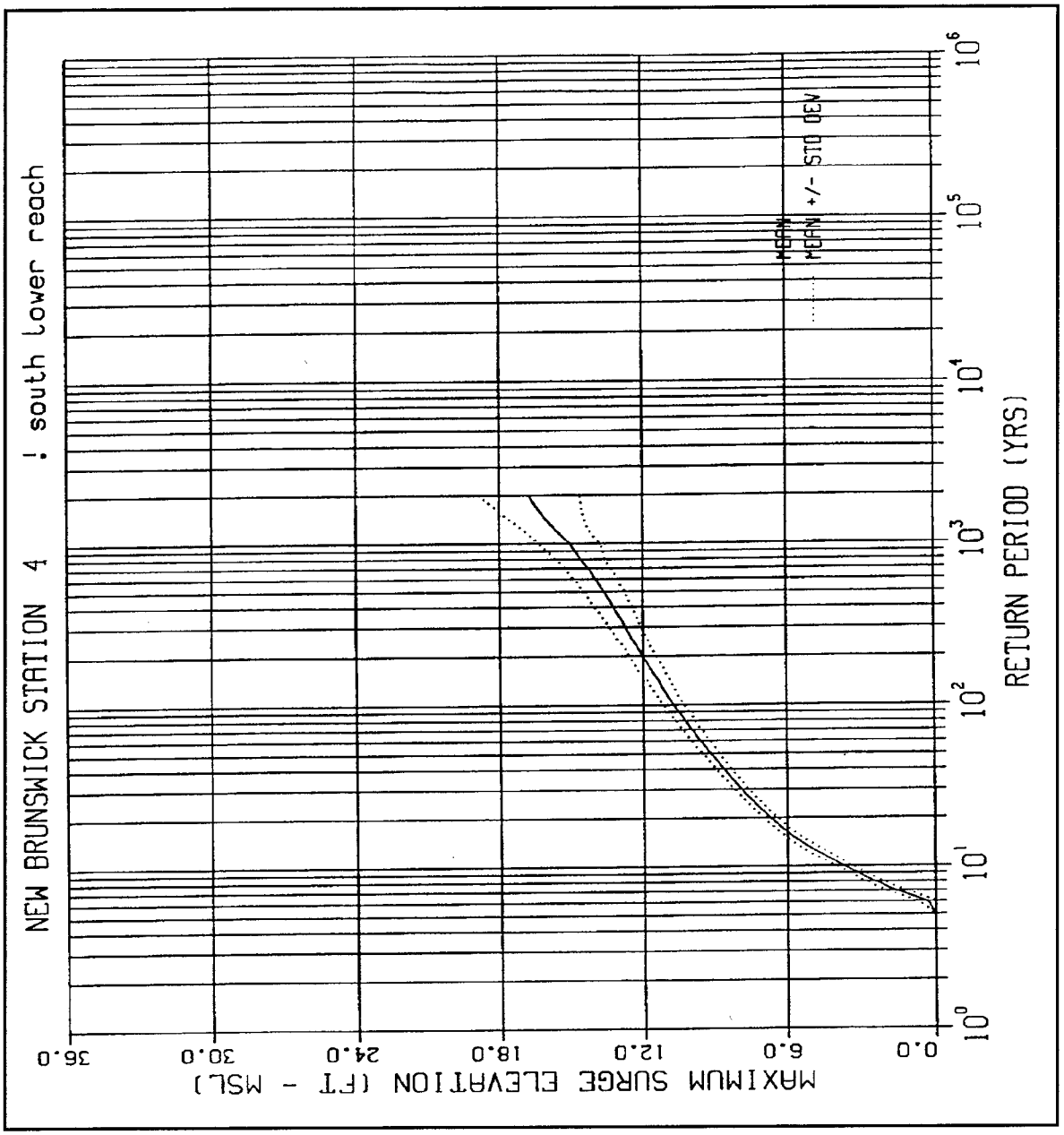

Figure B4. Stage-frequency relationship for Station 4

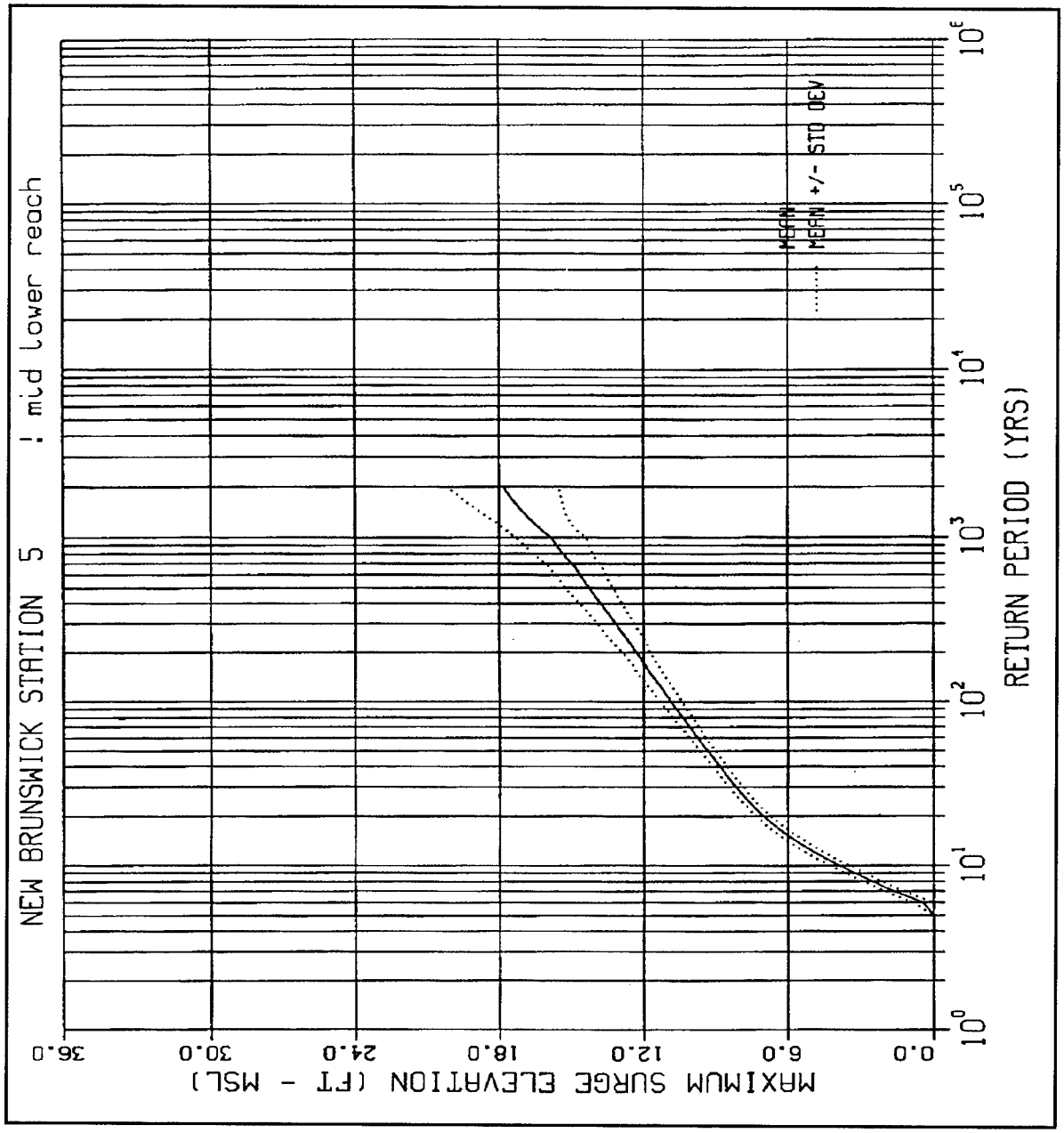

Figure B5. Stage-frequency relationship for Station 5

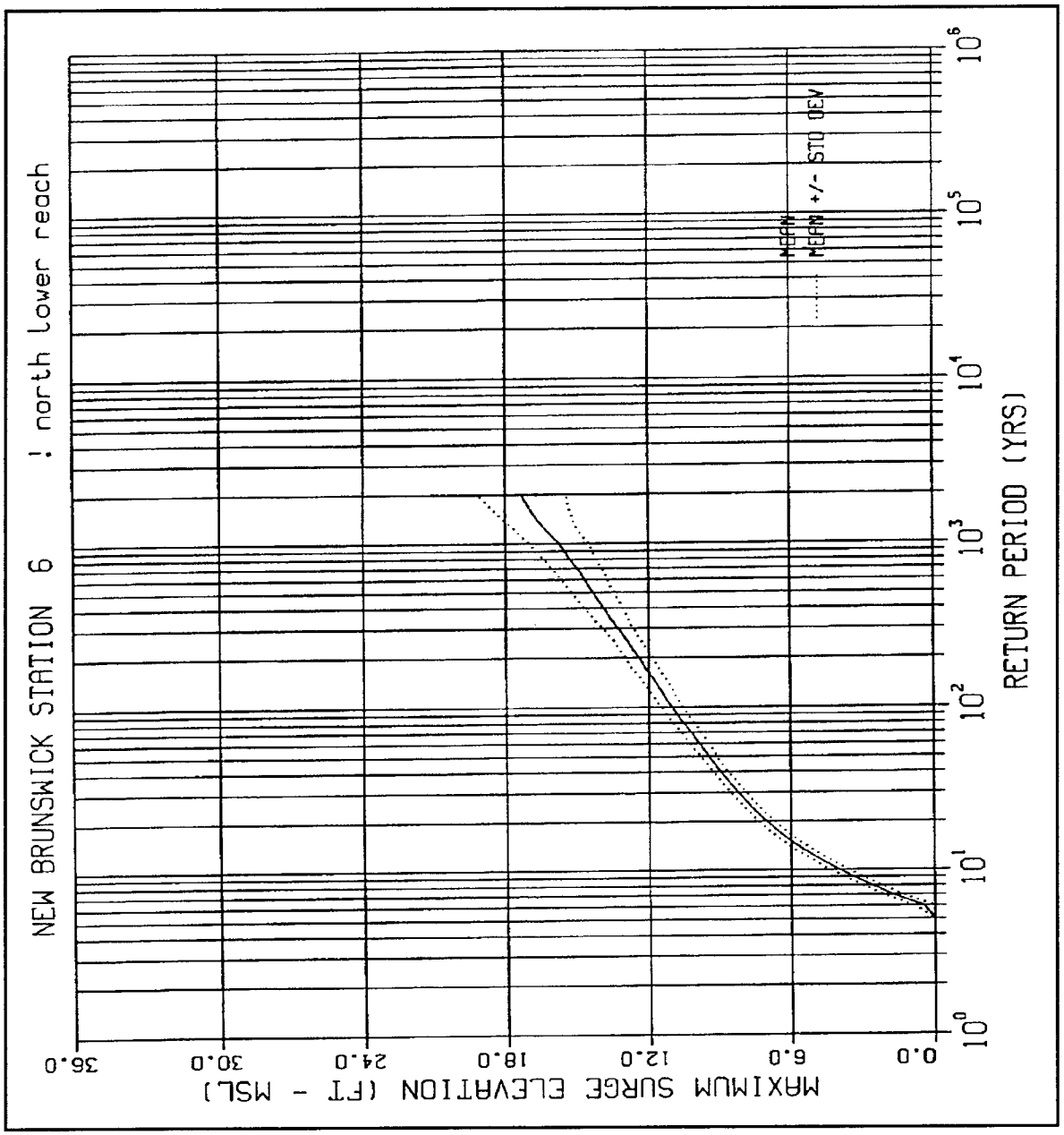

Figure B6. Stage-frequency relationship for Station 6

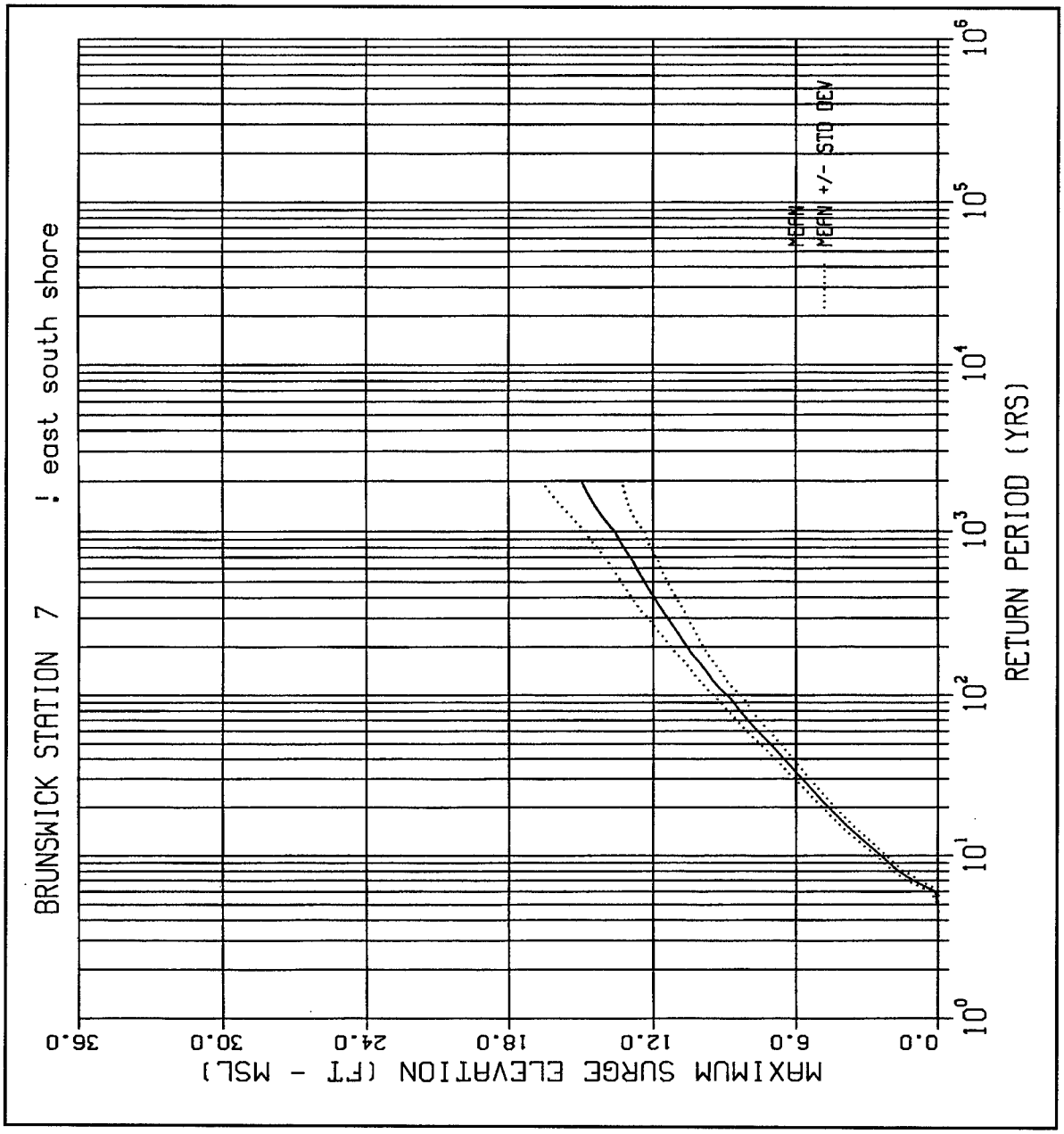

Figure B7. Stage-frequency relationship for Station 7

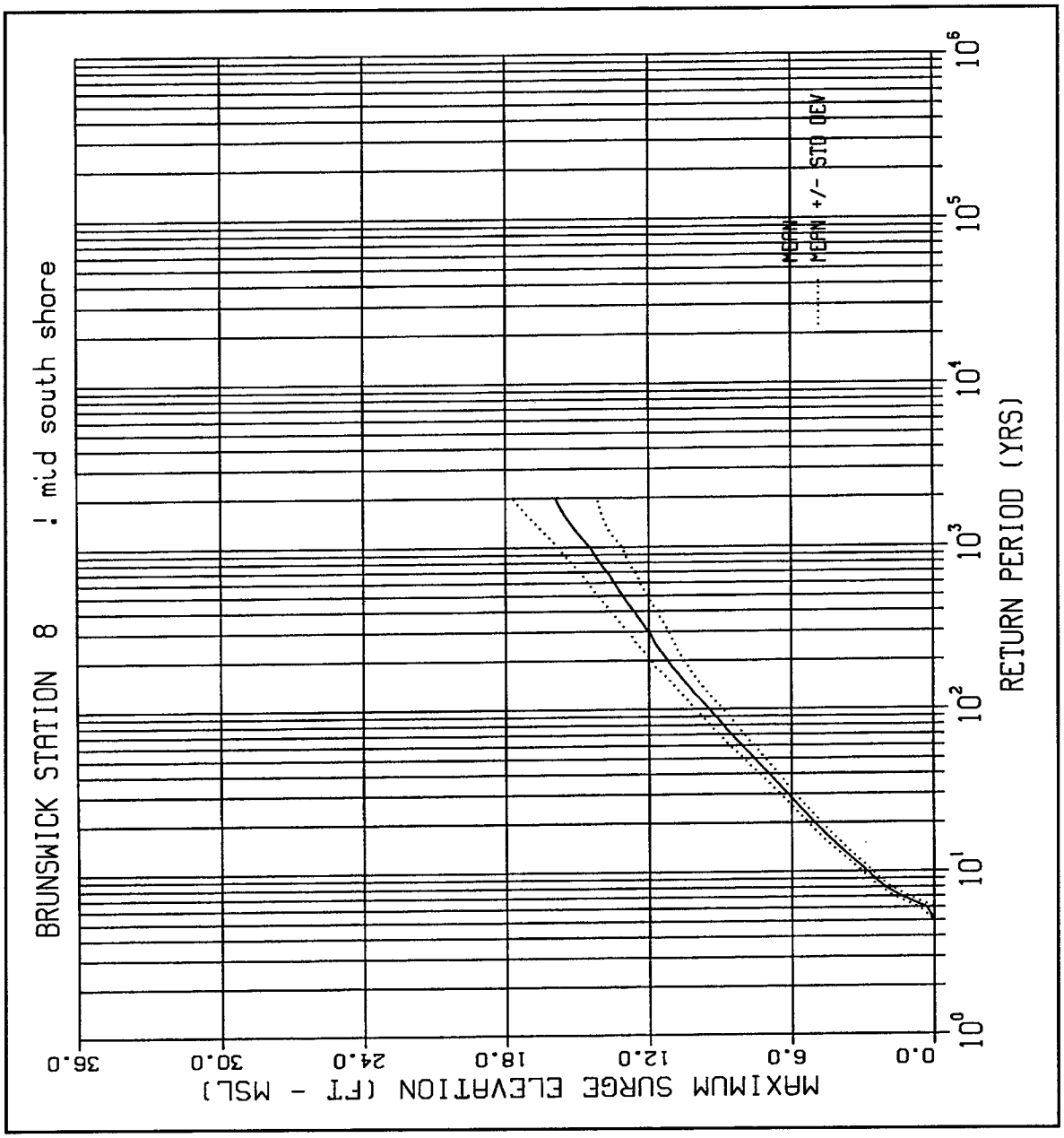

Figure B8. Stage-frequency relationship for Station 8

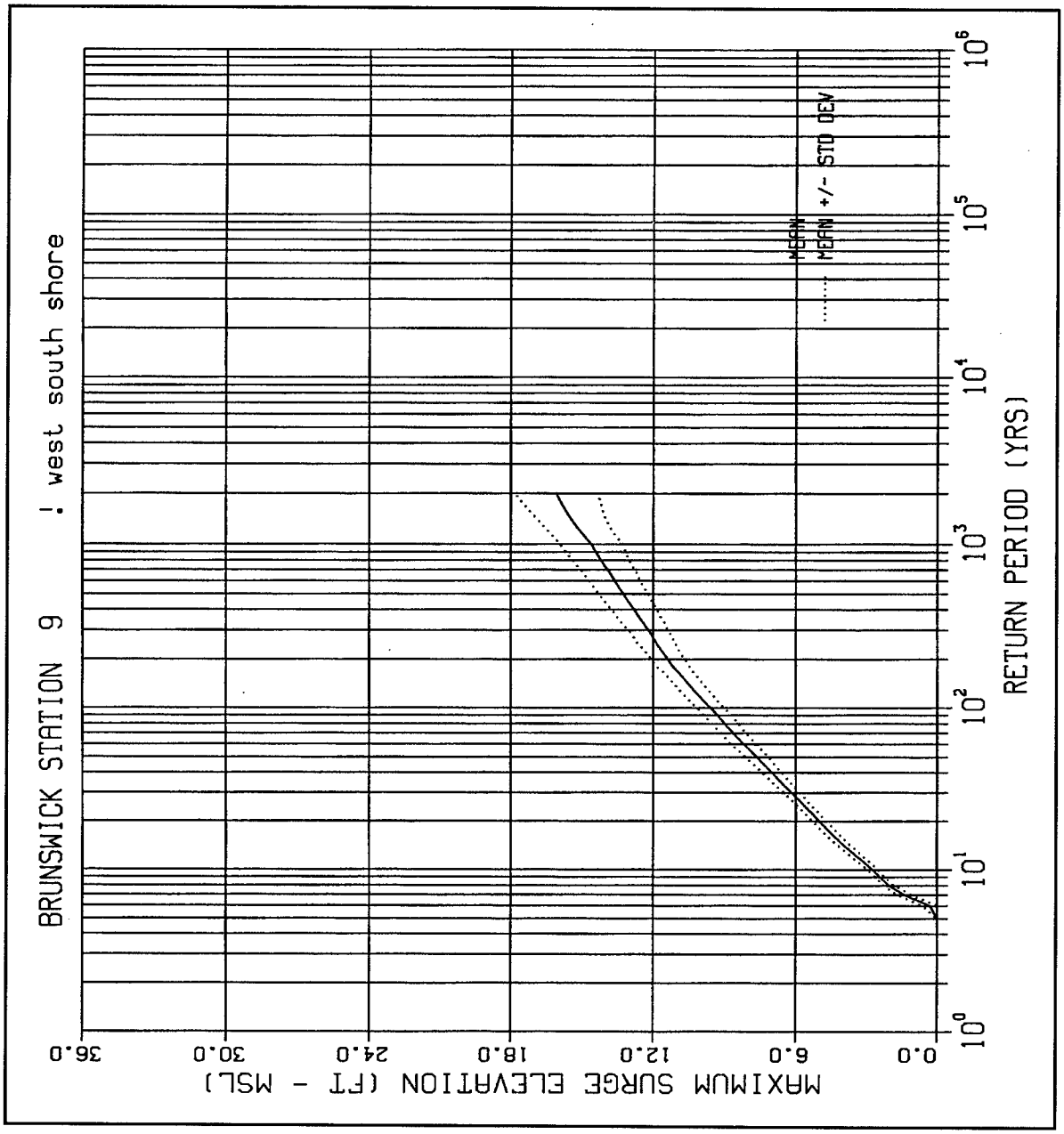

Figure B9. Stage-frequency relationship for Station 9

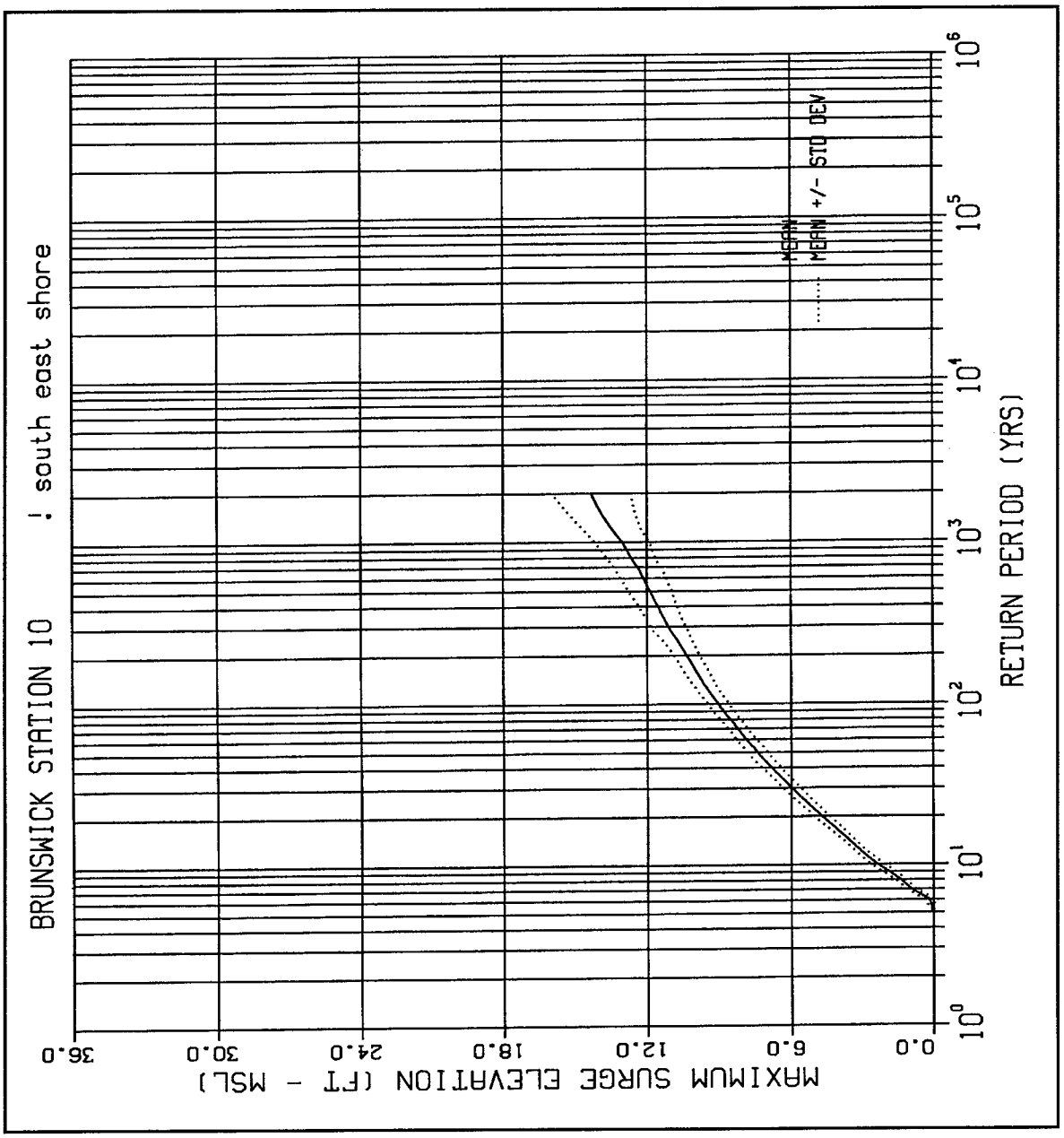

Figure B10. Stage-frequency relationship for Station 10

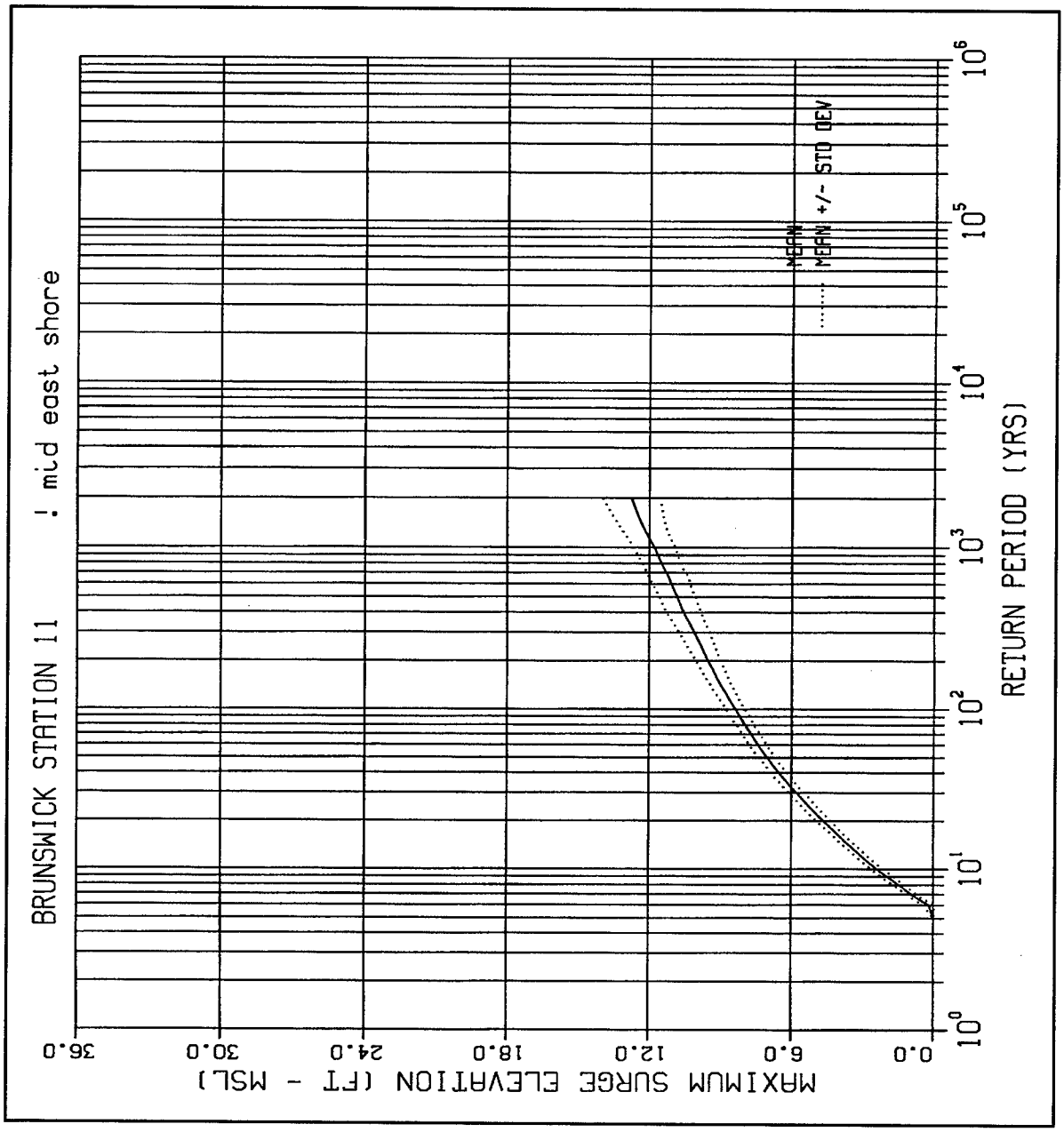

Figure B11. Stage-frequency relationship for Station 11

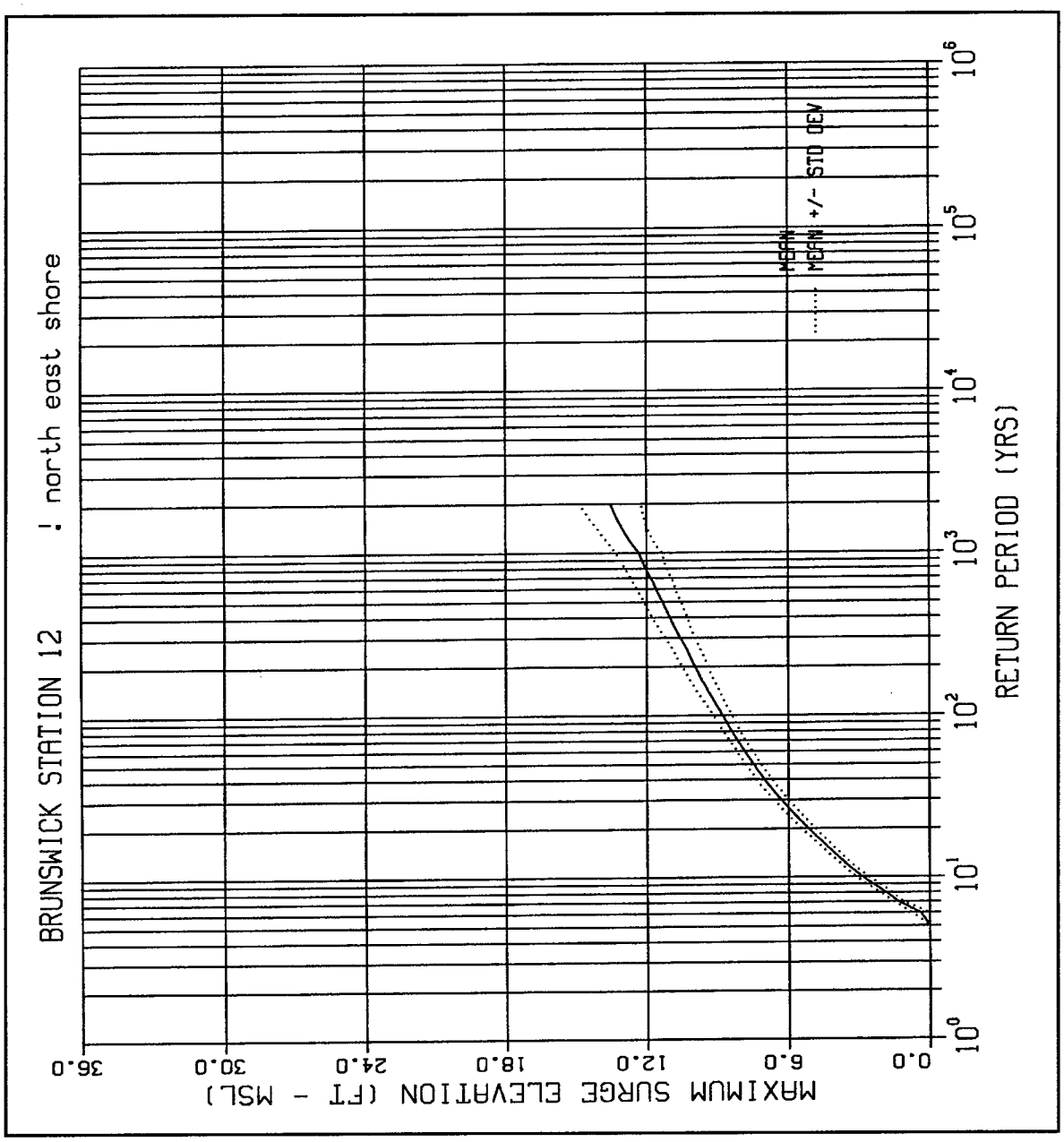

Figure B12. Stage-frequency relationship for Station 12

REPORT DOCUMENTATION PAGE

Form Approved
OMB No. 0704-0188

1. AGENCY USE ONLY *(Leave blank)*	2. REPORT DATE	3. REPORT TYPE AND DATES COVERED
	December 1999	Final report

4. TITLE AND SUBTITLE
Development of Water-Surface Elevation Frequency-of-Occurrence Relationships for the Brunswick, North Carolina, Nuclear Power Plant Site

5. FUNDING NUMBERS

6. AUTHOR(S)
Norman W. Scheffner, David J. Mark, Lihwa Lin,
Willie A. Brandon, Martin C. Miller

7. PERFORMING ORGANIZATION NAME(S) AND ADDRESS(ES)
Coastal and Hydraulics Laboratory
U.S. Army Engineer Research and Development Center
3909 Halls Ferry Road, Vicksburg, MS 39180-6199

8. PERFORMING ORGANIZATION REPORT NUMBER
Technical Report CHL-99-12

9. SPONSORING/MONITORING AGENCY NAME(S) AND ADDRESS(ES)
U.S. Nuclear Regulatory Commission
Washington, DC 20314-1000

10. SPONSORING/MONITORING AGENCY REPORT NUMBER

11. SUPPLEMENTARY NOTES

12a. DISTRIBUTION/AVAILABILITY STATEMENT
Approved for public release; distribution is unlimited.

12b. DISTRIBUTION CODE

13. ABSTRACT ***(Maximum 200 words)***

This report describes the procedure and results used in a hurricane stage-frequency analysis for the Brunswick Nuclear Power Plant Site using a statistical technique referred to as the empirical simulation technique (EST). This procedure, used for determining frequency-of-occurrence relationships, is a statistical resampling procedure that uses historical data to develop joint probability relationships among various measured storm parameters (e.g., maximum wind speeds). The resampling scheme generates large populations of data that are statistically similar to a much smaller database of historical events. Using this expanded data set, the EST generates a database of peak storm-surge elevations by simulating multiple-year periods (e.g., 2,000-year periods) of storm activity a multiple number of times.

The Brunswick study described in this report consisted of four interrelated tasks, each employing a separate numerical model. In the first task, historical hurricanes impacting the study area were analyzed to determine storm statistics. From these data, a set of hurricanes, representative of all storms impacting the area, were chosen and subsequently simulated with a tropical wind field model to generate wind and atmospheric pressure fields. Storm-surge events developed with the wind model output were simulated, in the second task, using a long-wave, finite-element-based hydrodynamic model to obtain peak storm-surge elevations. A spectral wind-wave model was employed to estimate wave setup in the third task. With the hurricane parameters serving as input to the wind field model, together with the corresponding total storm-surge elevations (combined storm surge, wave setup, and tide) predicted by the various models, statistical techniques are used for developing frequency-of-occurrence relationships in the fourth and final task.

14. SUBJECT TERMS

Frequency computations	Life-cycle simulations	Wave modeling
Hurricane modeling	Statistical modeling	
Hydrodynamic modeling	Storm surge modeling	

15. NUMBER OF PAGES
81

16. PRICE CODE

17. SECURITY CLASSIFICATION OF REPORT	18. SECURITY CLASSIFICATION OF THIS PAGE	19. SECURITY CLASSIFICATION OF ABSTRACT	20. LIMITATION OF ABSTRACT
UNCLASSIFIED	UNCLASSIFIED		